PROGRESS REPORT

CVD Polymers for Devices and Device Fabrication

Minghui Wang, Xiaoxue Wang, Priya Moni, Andong Liu, Do Han Kim, Won Jun Jo, Hossein Sojoudi, and Karen K. Gleason*

Chemical vapor deposition (CVD) polymerization directly synthesizes organic thin films on a substrate from vapor phase reactants. Dielectric, semiconducting, electrically conducting, and ionically conducting CVD polymers have all been readily integrated into devices. The absence of solvent in the CVD process enables the growth of high-purity layers and avoids the potential of dewetting phenomena, which lead to pinhole defects. By limiting contaminants and defects, ultrathin (<10 nm) CVD polymeric device layers have been fabricated in multiple laboratories. The CVD method is particularly suitable for synthesizing insoluble conductive polymers, layers with high densities of organic functional groups, and robust crosslinked networks. Additionally, CVD polymers are prized for the ability to conformally cover rough surfaces, like those of paper and textile substrates, as well as the complex geometries of micro- and nanostructured devices. By employing low processing temperatures, CVD polymerization avoids damaging substrates and underlying device layers. This report discusses the mechanisms of the major CVD polymerization techniques and the recent progress of their applications in devices and device fabrication, with emphasis on initiated CVD (iCVD) and oxidative CVD (oCVD) polymerization.

1. Introduction

1.1. Background of CVD Polymerization

As a mature technology, chemical vapor deposition (CVD) is widely employed in industry to produce inorganic thin films and materials (e.g., semiconductors and dielectrics for microelectronics, optoelectronics and energy conversion devices).[1,2] The CVD process is also one of the major techniques for synthesizing carbon nanotubes (CNTs) and graphene sheets.[3,4] More recently, the benefits of CVD have been demonstrated for creating and engineering polymer thin films.[1] In a typical CVD polymerization process, the vaporized monomers are introduced into a vacuum chamber and form polymer thin films on cooled substrates. The high-quality organic thin films and coatings derived from the aforementioned solvent-free and low-temperature process have found applications across a wide range of fields.[1] In a recent example, CVD-synthesized metal–organic covalent network (MOCN) thin films were demonstrated to display highly selective gas permeation and hence are excellent candidates for gas-separation membranes.[5] The surface energy modification enabled by CVD polymerization can create both hydrophilic anti-fouling surfaces[6–8] and hydrophobic icephobic/anti-hydrate surfaces.[9–12] Hydrophobic CVD polymers were also employed to enhance steam condensation efficiency.[13] CVD polymer functional surfaces have found utility in the fields of biomass extraction[14] and drug delivery.[15] In addition to the aforementioned applications, defect-free CVD insulating, semiconducting, and insulating polymers have proved valuable in the fabrication of organic electronic devices.[1,16–21]

Among various CVD polymerization techniques, two distinct solvent-free CVD polymerization processes, initiated chemical vapor deposition (iCVD) and oxidative chemical vapor deposition (oCVD), have been developed by Gleason and co-workers.[1,16,20,21] In an iCVD process, volatile monomer(s) (e.g., acrylates) and an initiator (e.g., tert-butyl peroxide, TBPO) flow into the vacuum chamber which has temperature controlled chamber walls and substrates. The initiator is then broken apart to form radicals by thermal decomposition,[8] UV radiation[22] or plasma initiation.[5] These radicals subsequently react with absorbed monomers on the cooled substrate to initiate the radical polymerization (chain growth mechanism) and form CVD polymers. In an oCVD process, the volatile monomer(s) (e.g., thiophene) and oxidant (e.g., iron III chloride) are introduced into the temperature controlled vacuum chamber followed by step-growth polymerization of conductive CVD polymers on the substrates.[23]

Aside from the iCVD and oCVD processes, plasma-enhanced chemical vapor deposition (PECVD), parylene CVD, molecular layer deposition (MLD), vapor deposition polymerization (VDP) and vapor phase polymerization (VPP) are additional common CVD polymerization processes.[1,16,20,21,24] PECVD and parylene CVD occur via a chain growth mechanism (radical polymerization), while in MLD, VDP and VPP, the monomers undergo a step-growth mechanism (condensation polymerization).

Dr. M. Wang, X. Wang, P. Moni, A. Liu, Dr. D. H. Kim, W. J. Jo, Dr. H. Sojoudi, Prof. K. K. Gleason
Department of Chemical Engineering
Massachusetts Institute of Technology
77 Massachusetts Avenue, Cambridge
MA 02139, USA
E-mail: kkg@mit.edu
Dr. H. Sojoudi
Department of Mechanical
Industrial & Manufacturing Engineering
The University of Toledo
Toledo, Ohio 43606, USA

**ADVANCED
SCIENCE NEWS**
www.advancedsciencenews.com

**ADVANCED
MATERIALS**
www.advmat.de

PROGRESS REPORT

Differences in polymerization mechanisms have implications for which monomers can be employed with a specific process and hence the types of polymers can be formed by a given approach.

In a PECVD process, monomers are fragmented by plasma to form a variety of radical species. The resulting thin films are often highly crosslinked,[25] and thus can be mechanically and thermally robust. However, the properties of the PECVD films can also be negatively impacted by the loss of desirable organic functional groups and by defect formation resulting from the plasma fragmentation.[26] For example, recently it has been demonstrated that PECVD films displayed reduced photo-stability as compared to that of iCVD films grown using the same monomer.[25]

Instead of using a plasma as the energy source, parylene CVD employs heat to crack vapor phase reactants related to [2,2]paracyclophane. Polymerization of the resulting radical species on cooled substrates proceeds via a chain growth mechanism.[27] By varying the functional groups attached to the [2,2]paracyclophane, polymer films with high retention of functionality can be produced via the parylene CVD process and an impressive range of applications has been demonstrated.[27–30]

In the MLD[31] and VDP[32] processes, bifunctional monomers are necessary to participate in condensation polymerization. The resulting polymers generally fall into a distinctly different class of chemical structures from macromolecules grown by free radical means. Unlike VDP, in which multiple monomer species flow into the reactor simultaneously, in MLD, flows of different monomers are alternated under conditions where growth is self-limited. The VPP process was occasionally termed as VDP process in some literature.[24] In this report, we use VPP to refer to a process related to the oCVD process for forming conjugated polymer thin films. While, both VPP and oCVD utilize vapor phase monomers, the difference is that in VPP, a low-volatility oxidant is applied to the substrate as a solid, whereas a vapor phase oxidant is employed in oCVD.

It should be noted that the CVD polymerization techniques are distinctively different from the thermal- or laser-based physical vapor deposition (PVD) processes (e.g., matrix assisted pulsed laser evaporation, MAPLE) for polymeric film formation.[33,34] In a PVD process, pre-synthesized polymers, as opposed to the monomers, are typically employed for film formation. Typically, PVD provides line-of-sight coverage of non-planar features, in contrast to the conformal coverage possible with CVD. The scope of this progress report will focus on CVD polymers related applications.

1.2. CVD Polymers for Organic Devices and Device Fabrication

Organic devices have attracted significant attention in the past decades for enabling large-area, mechanically flexible and low-cost electronics.[35] Organic devices, including displays and photovoltaics, have been are produced by traditional solution processes. This approach requires significant interfacial optimization to avoid dewetting behavior that leads to pinhole defects and thus limits the ability to produce ultrathin films. Additionally, it is challenging to achieve conformality (i.e., to have the same film thickness over all the features of a geometrically

Minghui Wang is currently a postdoctoral associate in Prof. Karen K. Gleason's research group in the Department of Chemical Engineering, Massachusetts Institute of Technology. His research mainly focuses on the CVD-enabled surface modification for fouling and scaling control in the desalination processes, and CVD-synthesized gas-separation films. He received his B.S. in Chemistry from East China Normal University in 2005, his M.S. in materials chemistry and physics from Shanghai Institute of Ceramics, Chinese Academy of Sciences in 2008, and his Ph.D. in polymer science and engineering from Lehigh University in 2014 (advisor Prof. Steven L. Regen).

Xiaoxue Wang is currently pursuing her Ph.D. in chemical engineering under the supervision of Professor Karen Gleason at Massachusetts Institute of Technology. Her research interests mainly focus on the electrical, optical and other properties of the conjugated polymers synthesized by oCVD technology, and their applications in electronic devices such as gas sensors, LEDs, and solar cells. She received her B.S. degree from the Department of Chemical Engineering at Tsinghua University, China in 2012 with her bachelor thesis on the computational design of enzymes.

Priya Moni is currently pursuing her Ph.D. in materials science and engineering under the supervision of Professor Karen Gleason at the Massachusetts Institute of Technology. Her current research focuses on using iCVD and oCVD techniques to fabricate activated layers for microscale lithium-ion batteries and facilitate sub-10 nm patterning for integrated circuits. She obtained her B.S.E. in materials science and engineering from the University of Michigan in 2013.

complex device) via solution-based method.[17] Conformal coverage is particularly important for device structures having high-aspect-ratio features, including nanostructured devices

such as 3D batteries and ultracapacitors.[20,36] A second issue within the solution-based processing methods is the limited solubility or complete insolubility of some target polymers. Indeed, to enhance the solubility of these polymers, additional synthetic modifications to attach pendant groups to the target structures are commonly practiced, which increase the complexity of device fabrication.[20] These are two of the factors have limited the application of solution-based methods in the field of device fabrication. As a result, technologies that can avoid solvent–substrate interactions are desirable.

In this regard, CVD techniques introduced in the background are particularly suitable for integration into devices and processes for fabricating devices owing to their unique characteristics, including: i) solvent-free, ii) low temperature, iii) conformal deposition, iv) precise thickness control from nanometers to micrometers, v) versatile functionality due to the large selection of precursor library, and vi) readily scalable for large area depositions (**Figure 1**).[1,16,20,21] These CVD processes provide excellent compatibility to a wide range of substrates since there is no potential for solvent or plasma damage of the underlying material. The absence of wettability and surface tension renders CVD "substrate independent", meaning that modification of the process is not required for each different substrate. This substrate independence reduces device fabrication complexity and expands the applicability of the CVD method to novel substrates. The solvent-free nature also assures minimal dewetting and essentially pinhole free CVD polymer films.[37] CVD polymer composition and crosslinking can be systematically tuned by introducing co-monomers, which can further optimize device performance and enhance the device durability and stability. In addition, avoiding toxic organic solvents can lead to cost reduction and greener chemistry, while avoiding the problem of having residual solvent in the device layers.
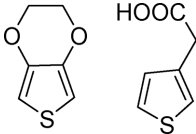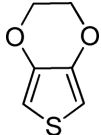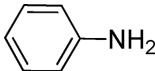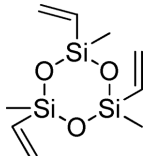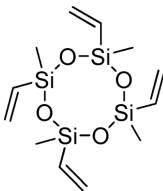
A second major advantage of the CVD polymerization is its conformal deposition with excellent thickness control. For electronic or sensing devices having high-aspect-ratio features, conformal coatings are crucial to enable a consistent performance and to avoid the failure of the device. A third advantage of CVD poly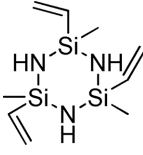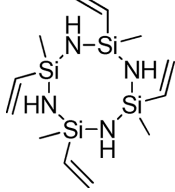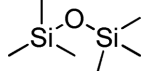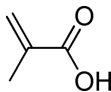merization is the low temperature involved in the polymerization process. This characteristic allows direct deposition of polymer thin films on fragile substrates (e.g., papers, fabrics) without additional steps (e.g., transfer).[38,39] In addition, the versatility in the CVD precursor choices and the ability to fully retain functionality of precursors in the final CVD polymers allow the technique to be integrated into a large selection of device fabrication processes. Last but not the least, it should be noted that CVD polymerization can also be scaled up for commercialization via large area batch and roll-to-roll processes.[39] As a result, iCVD and oCVD derived polymer thin films have the potential to be integrated into a wide variety of optoelectronic devices and into the process utilized to fabricate these devices.

The purpose of this progress report is to cover recent developments involving the application of CVD polymer thin films in the field of device fabrication. The key advantages of CVD polymers and the links to devices and device fabrication are summarized in Figure 1. This report will emphasize publications appearing in the last 24 months, since prior reviews have provided discussions and summaries of previous accomplishments on this topic.[1,16,20,21,40] The specific categories of devices will be divided into chemical and bio-sensors; electrochemical energy-storage elements; electronic devices for logic and memory; photonic devices and advanced printing. The final section will focus on the use of CVD polymers to enhance the fabrication of devices through advanced patterning. The CVD polymers discussed in this report are summarized in **Table 1**.
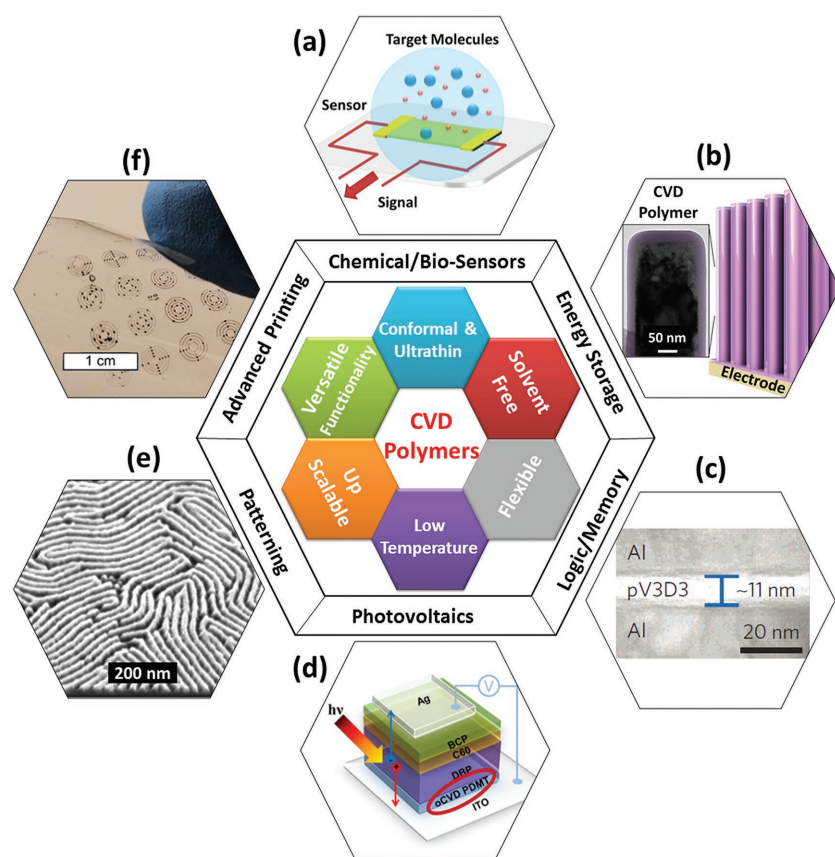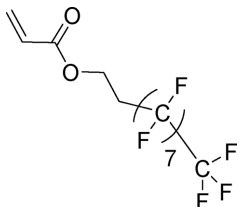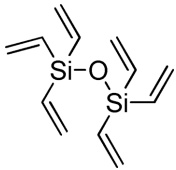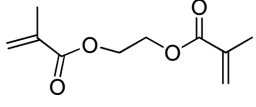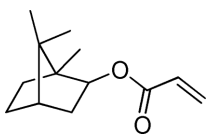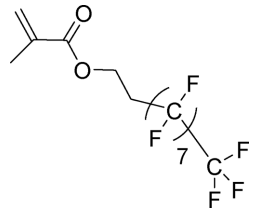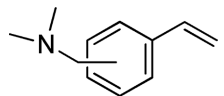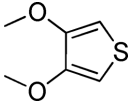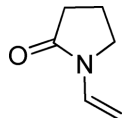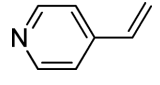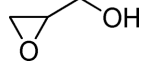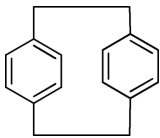

Figure 1. Unique features of chemical vapor deposition (CVD) polymers, and their applications in devices and device fabrication: a) schematic of a sensor; b) schematic of a 3D battery, the inset shows the TEM image of a silicon nanowire coated with ultrathin and conformal CVD polymer coating; Si nanowire arrays obtained from the group of Prof. C.V. Thompson at MIT; c) Cross-sectional TEM of an ultrathin (11 nm) iCVD dielectric between two aluminum electrodes forming a MIM device;[17] d) schematic of photovoltaic structure with oCVD poly(3,4-dimethyoxythiophene) (PDMT) integrated in the device;[19] e) SEM image shows the sub-10 nm patterns in silicon dioxide enabled by an iCVD top coating technique;[41] and f) flexoprinting of electronic features on PET substrates, enabled by conformal CVD coating of a hydrophobic polymer onto arrays of patterned carbon nanotubes (CNTs). c) Reproduced with permission.[17] Copyright 2015, Nature Publishing Group. d) Reproduced with permission.[19] Copyright 2016, Wiley-VCH.

Table 1. A summary of CVD polymers appeared in this report.
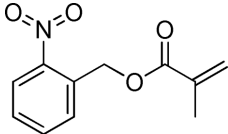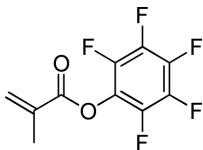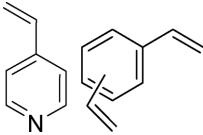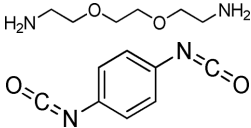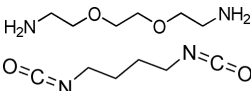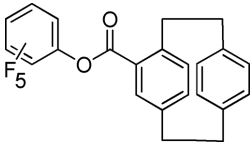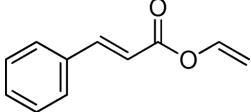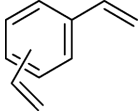
Polymer	Monomer(s)	Technique	Application	Ref.
Poly(3,4-ethylenedioxythiophene-co-3-thiophene acetic acid), p(EDOT-co-TAA)		oCVD	Chemical sensors, biosensors	[42–44]
Poly (3,4-ethylenedioxythiophene), PEDOT		oCVD	Supercapacitors, Sensors, electrochromics	[18,45–48]
Poly(pyrrole), Ppy		VPP	Supercapacitors, sensors	[49–51]
Polyaniline		VPP	Sensors	[24]
Poly(thiophene), PTh		oCVD	Supercapacitors	[52]
Poly(1,3,5-trimethyl-1,3,5-trivinyl-cyclotrisiloxane), pV3D3		iCVD, electro-polymerization	Lithium-ion batteries	[16,36,53]
Poly(2,4,6,8-tetramethyl-2,4,6,8-tetravinylcyclotetrasiloxane), pV4D4		iCVD, hybridized with ALD film	Biosensors, gate dielectric, barrier layer, encapsulation for electronics, Li ion batteries	[16,17,36,37,54–56]
Poly(1,3,5-trimethyl-1,3,5-trivinyl-cyclotrisilazane), pV3N3		iCVD	Lithium-ion batteries	[16,36]
Poly(1,3,5,7-tetramethyl-1,3,5,7-tetravinyl-cyclotetrasilazane), pV4N4		iCVD	Lithium-ion batteries	[16,36]
Poly (hexamethyldisiloxane), pHMDS		PECVD	Proton exchange membranes, fuel cells	[57]
Poly (methacrylic acid), pMAA		PECVD, iCVD	Proton exchange membranes, fuel cells	[57–59]

Table 1. Continued.

Polymer	Monomer(s)	Technique	Application	Ref.
Poly(1H,1H, 2H, 2H-perfluorodecylacrylate), pPFDA		iCVD	Proton exchange membranes, fuel cells, gate dielectric, water-repellent and self-cleaning surfaces, Microfluidic devices	[58–63]
Poly(hexavinyldisiloxane), pHVDS		iCVD	Barrier layer, lithium-ion batteries	[64,65]
Poly(ethylene glycol dimethacrylate), pEGDMA		iCVD	Gate dielectric	[60]
Poly(isobornyl acrylate), pIBA		iCVD	Gate dielectric	[60]
Poly(3,3,4,4,5,5,6,6,7,7,8,8,9,9,10,10,10-heptadecafluorodecyl methacrylate), pPFDMA		iCVD	Water repellent encapsulation layer for electronics	[54]
Poly(dimethylaminomethyl styrene) (PDMAMS), pDMAMS		iCVD	Work function modification, electron transporting polymer for electronics	[66]
Poly(3,4-dimethoxythiophene), PDMT		oCVD	Neutral hole transporting polymer for electronics	[19]
Poly(vinylpyrrolidone), pVP		iCVD	Oxygen and moisture barrier for organic electronics	[67]
Poly(4-vinylpyridine) (P4VP)		iCVD	Oxygen and moisture barrier for organic electronic devices, photoresist	[67,68]
Polyglycidol		iCVD	Oxygen and moisture barrier for organic electronics	[69]
Poly (para-xylyene), PPX		parylene CVD	Membrane	[30,70]

Table 1. Continued.

Polymer	Monomer(s)	Technique	Application	Ref.
Poly(ortho-nitrobenzyl methacrylate), PoNBMA		iCVD	Biosensor	[63]
Poly(pentafluorophenl methacrylate), pPFM		iCVD	Biosensor	[63]
Poly(4-vinyl pyridine-co-divinylbenzene), p(4VP-co-DVB)		iCVD	Sensor	[61]
Polyurea 1		MLD	Photoresist	[71]
Polyurea 2		MLD	E-beam resist	[72]
Poly(p-xylyele-4-carboxylic acid pentafluorophenolester-co-p-xylyene)		parylene CVD	Cell culture platform	[73]
Poly(vinyl cinnamate), pVCin		iCVD	Photoresist	[74]
Poly(divinylbenzene), pDVB		iCVD	Topcoat for patterning	[41]

2. Chemical and Biological Sensing

Oxidative chemical vapor deposition (oCVD) is an efficient method to synthesize conjugated polymers including, but not limited to, polythiophene, polypyrrole, and polyselenophene.[1] The process of oCVD has been well described previously.[1] In a typical oCVD process, vapors of the oxidant (e.g., FeCl₃) and the monomers (EDOT, thiophene, etc) are simultaneously introduced into a vacuum chamber. The polymer synthesis takes place on a substrate affixed to a temperature controlled stage, where the precursors adsorb from the vapor phase. oCVD has the advantages of being solvent-free, easily tailored, utilizes low operational temperatures, and produces conformal coatings on ultrafine structures.[1] In addition, utilizing conjugated monomers to which functional groups have been added, the oCVD technique is capable of introducing various functional groups into electrically conducting polymer.[44,75] The added functional groups can be used for covalently tethering sensing elements (e.g., metal nanoparticles,[43] proteins,[76,77] etc), and therefore provide a versatile platform for chemical and biological sensing. Together with the electrical conducting nature of oCVD films, all of these advantages make oCVD technique a very powerful tool for fabricating chemical and biological detectors based on responses in electrical resistance. Such resistive sensing is desired for applications in which low cost and low weight are essential.

Initiative chemical vapor deposition (iCVD),[1] a technique introduced in previous sections, is also a very useful tool in

chemical and biological sensing. As a vapor phase polymerization technique, iCVD is also capable of synthesizing conformal coatings on nanostructures.[1,56] Based on the physical properties of the coating layer, iCVD polymers can function as selective layers for gas sensors.[18] Furthermore, polymers containing useful functional groups for sensing element attachment can also be easily achieved using iCVD technique.[56] By providing a filter layer or a docking location for sensing elements such as DNA primers, the iCVD technique also finds wide applications in chemical/biological detection.[56]

The utility of oCVD and iCVD for chemical sensing has been demonstrated for volatile organic compounds (VOCs) detection at room temperature. VOCs are widely known as safety hazards for industrial plants, particularly in oil refineries.[44] Among all the possible sensor types, chemiresistors, sensors displaying resistive response after exposure to an analyte, are one of the best candidates for integration onto printed circuit boards and into wireless networks. However, traditional metal oxide chemiresistive sensors require high operational temperatures (200–400 °C). The energy consumption of the required heating elements[44] is a significant barrier for integration into a wireless sensor network. A variety of chemiresistive sensing strategies for ambient temperature VOC detection have been demonstrated using oCVD and iCVD techniques. By avoiding the need for a heating element and the associated energy use, these CVD polymer-based sensors pave the way for integration into wireless sensor networks.
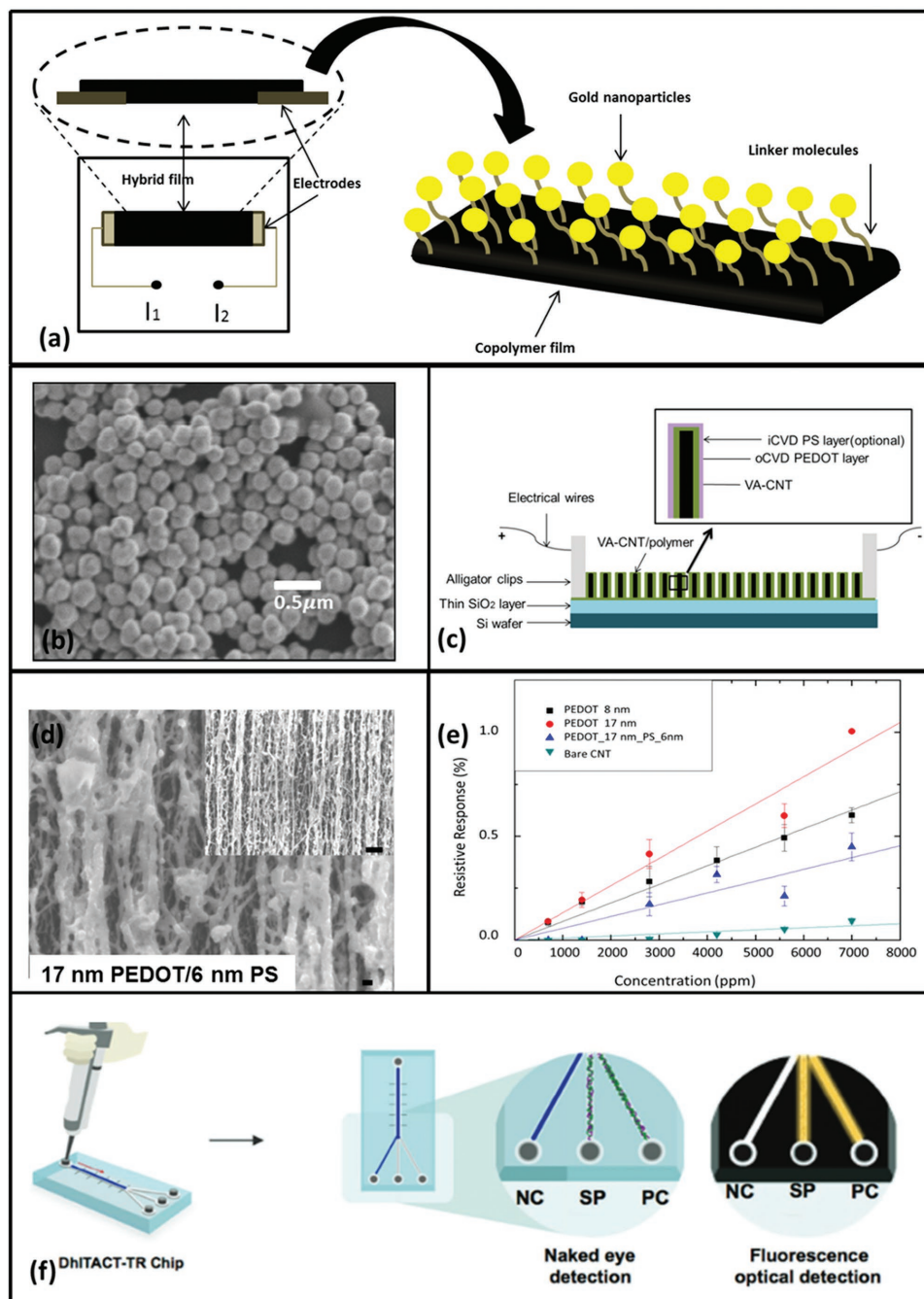
Sreeram et al.[42,43] and Bhattacharyya et al.[76,77] demonstrated the utility of oCVD electrically conducting polymers with –COOH functional groups to immobilize detection elements such as metal nanoparticles and enzymes. Specific binding of an analyte to the detection element results is transduced into a change in electrical resistance of the CVD organic conductor. Resistance changes as large as 6% have been reported. From that work, Wang et al.[44] developed a methanol vapor sensor based on Au nanoparticles tethered via the same carbodiimide chemistry. As shown in **Figure 2**a, gold nanoparticles are immobilized on oCVD poly(3,4-ethylenedioxythiophene-*co*-3-thiophene acetic acid) (poly(EDOT-*co*-TAA)) with a linker molecule 4-aminothiophenol. The scanning electron micrograph (SEM) in Figure 2b clearly shows the existence of gold nanoparticles after rigorous rinsing. With a positive resistive response generated by the work function modulation, the detector demonstrates a detection limit of ≈171 ppm for methanol vapors. In addition, all the sensing materials were fabricated directly on a printed circuit board, which made it compact and easy to be integrated into a sensor reading board. The selectivity of the device is also demonstrated over n-pentane.

Another promising chemiresistive detector is the vertically aligned carbon nanotube (VA-CNT)/oCVD/iCVD sensor shown in Figure 2c.[18] Ultrathin (<17 nm thick) oCVD poly(3,4-ethylenedioxythiophene) (PEDOT) coatings were synthesized directly on VA-CNT arrays.[18,45,46] An iCVD polystyrene layer was added as a semipermeable skin layer in order to enhance the selectivity of the device. Conditions were used to achieve both oCVD and iCVD polymer coatings around each individual tube in the array, so-called conformal coating, as opposed to creating a blanket films of polymer on top of the CNT forest. Previously, sensors based on CNTs and conducting polymer

nanowires have drawn great attention because of their high sensitivity and versatile detection ability.[78,79] The hybrid device combines the merits of both kinds of sensors and provides a better measuring method and a simplified fabrication scenario.[18] The SEM image in Figure 2d shows the oCVD/iCVD polymer coated VA-CNT. The performance of these devices can be found in Figure 2e. With good sensitivity and very low noise, the device effectively detects non-polar n-pentane, while giving a negative response to methanol vapors, which is in agreement with the expected response.[78] Electrical conduction mechanisms based on inter-tube electron hopping and intra-tube Fermi level modulating are proposed to explain the experimental results.[18] Additionally, with a layer of iCVD polystyrene, the selectivity of n-pentane versus methanol vapor is greatly enhanced. The compact device operating at room temperature is a good candidate for a sensing element in a wireless network.

A different technology, vapor phase polymerization (VPP), is also often used to synthesize conducting polymers as the sensing layer of chemiresistive sensors. Danesh et al. reported an ammonia sensor based on VPP polyaniline.[24] At the bottom of the sensor is a heating plate in order to operate at elevated temperatures and further enhance the ammonia sensing performance. Separated from the hot plate by a thin dielectric film are the interdigitated electrodes (IDEs) in order to measure the resistance change of the polyaniline film above. The precursor, solution of oxidant and the dopant poly(4-styrenesulfonic acid), is first spin coated on the interdigitated electrodes. Later, the monomer, aniline is introduced into a hot chamber via vapor phase. The polymerization takes place on the device directly by adsorption of monomer molecules. With a heating plate, the device is able to detect as low as 350 ppb of ammonia. Using a similar polymerization technique, Alizadeh et al.[51] reported a room temperature VOC sensor based on polypyrrole (PPy). In this work, the solution of Fe(III) chloride was first spread on Cu-IDEs, and the pyrrole vapor is introduced for PPy film growth. Their sensor detects a variety of VOCs such as organic solvent vapors.

The merit of iCVD conformal coating on fine structures provides the possibility of applying this technique on microchannels as docking sites for immobilizing DNA primers.[56] Jung et al.[56] recently developed an optical Middle East Respiratory Syndrome (MERS) detection platform based on iCVD coatings. The MERS outbreak in 2015 in the Republic of Korea profoundly affected the life quality for numerous people. Faster detection of the MERS coronavirus is therefore greatly needed. The current polymerase chain reaction (PCR) detection method is very accurate;[56] however, it is very time-consuming and requires well trained professionals. The researchers developed a new platform called DhITACT-TR based on iCVD and microfluidic technologies as seen in Figure 2f. iCVD was used to synthesize a conformal coating of poly(2,4,6,8-tetramethyl-2,4,6,8-tetravinylcyclotetrasiloxane) (PV4D4)[1,56] on a pre-fabricated channel. DNA primers end-functionalized with –SH are covalently tethered on the polymer coating via a thiol-ene click reaction. The immobilized DNA primer is further used to hybridize and immobilize different DNA templates for negative control and positive control. The DhITACT-TR system is able to detect the MERS coronavirus within 30 min at a very low pathogen

ADVANCED
SCIENCE NEWS
www.advancedsciencenews.com

ADVANCED MATERIALS
www.advmat.de

PROGRESS REPORT

Figure 2. a) The structure of an oCVD/Au nanoparticle sensor directly synthesized on a printed circuit board;[44] b) SEM image of the covalently tethered Au nanoparticles on the oCVD copolymer surface;[44] c) the structure of the sensing material based on vertically aligned carbon nanotube (VA-CNT) arrays and oCVD/iCVD coatings;[18] d) the SEM image of the polymer coated VA-CNT arrays as sensing element, the scale bars in the main figure and in the inset are 100 nm and 1 μm respectively;[18] d) the performance of the CNT sensor on n-pentane at various concentrations;[18] f) a DhITACT-TR chip based on iCVD PV4D4 coating for MERS coronavirus detection.[56] a,b) reproduced with permission.[44] Copyright 2015, American Chemical Society; c,d,e) reproduced with permission.[18] Copyright 2016, American Chemical Society; f) reproduced with permission.[56] Copyright 2016, Wiley-VCH.

concentration, which is much more efficient compared to the traditional PCR technique. In addition, the sensitivity is enhanced by 100 fold compared to their last generation of detection chips. Furthermore, the platform with iCVD coatings is capable for detection of various infectious diseases.[56]

3. Electrochemical Devices

As devices, such as sensors and actuators, miniaturize and approach the microscale, development of power supplies that maintain device portability within a small volume is an

increasingly pressing need. Several electrochemical energy-storage methods, such as proton exchange membrane fuel cells (PEMFCs), lithium-ion batteries, and supercapacitors have the potential to be miniaturized. Both iCVD- and oCVD-synthesized polymers can aid the creation of the aforementioned mini and micro power supplies.

3.1. Proton Exchange Membrane Fuel Cells

Proton exchange membrane fuel cells are attractive as clean energy generation devices since their only byproduct during use is water. The polyelectrolyte, or proton exchange membrane (PEM), is a critical component which serves to transport protons from the anode to the cathode. PEMs with both hydrophobic and hydrophilic moieties allow for controlled uptake of water with good proton conduction. Dupont Nafion®, a perfluorinated sulfonic acid polymer, is the current industrial standard. However, its production method results in high costs and difficulties for integration into mini devices.

To address these deficiencies, development of alternative PEMs through iCVD and plasma-enhanced CVD (PECVD) has been studied. Dupont Nafion® facilitates proton transport by created hydrophilic water channels in a hydrophobic matrix. In an attempt to replicate this structure, Coclite et al.[59] studied the deposition kinetics of the copolymer formed from 1H,1H,2H,2H-perfluorodecyl acrylate (PFDA) and methyacrylic acid (MAA) as well as the resulting chemical composition and morphological structure of p(PFDA-co-MAA).

Reactivity ratios $r_{MAA} = 0.85$ and $r_{PFDA} = 0.39$ indicate moderate alternating copolymer behavior, which is important for controlled water uptake. The crystal structure of p(PFDA-co-MAA) was further studied by Ranacher et al.[58] Various X-ray techniques revealed that p(PFDA-co-MAA) crystallizes in a smetic A bilayer structure. An increase in MAA content increases the interplanar spacing to form water transport channels as seen in **Figure 3**a. Further increases in MAA content result in completely amorphous films. Correspondingly, the proton conductivity of p(PFDA-co-MAA) increases with MAA content, peaking at 55 S cm^{-1} for 41% MAA content. For comparison, the proton conductivity of Dupont Nafion is approximately 100 S cm^{-1}. Further work by Urstoger et al. sought to reduce swelling of PEMs after extended water exposure.[57] PECVD was used to create crosslinked pMAA using hexamethyldisiloxane (HMDSO). pMAA homopolymer films either swelled or shrunk as much as 26% after two weeks exposure to water. Copolymer films deposited at higher plasma power showed greater stability with only 4% shrinkage after the same water exposure. The proton conductivity of these films was approximately 1 mS cm^{-1}, much lower than the previous p(PFDA-co-MAA) films.

3.2. Lithium-Ion Batteries

Rechargeable lithium-ion batteries have been studied for their higher energy densities compared to other battery chemistries. iCVD polymer films have found applications in both macroscale and microscale devices.
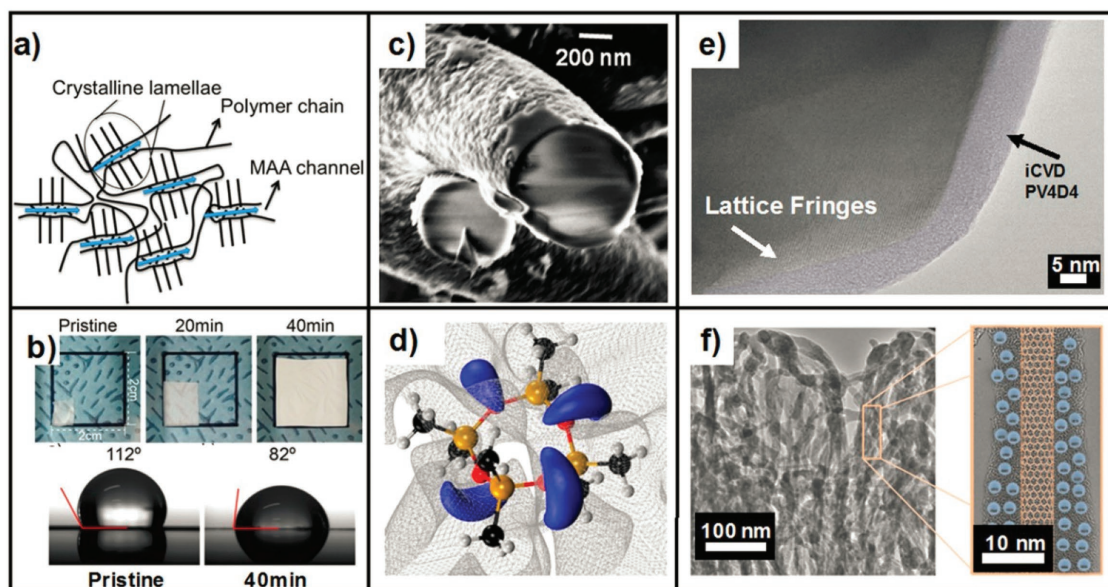
Figure 3. a) Schematic of crystalline PFDA domains with MAA proton conduction channels;[58] b) top: thermal shrinkage of PE separators with and without iCVD coatings, bottom: water contact angle on separator with and without iCVD coatings;[64] c) SEM cross section of conformal iCVD pV3D3 coated on C@SiO$_2$ fiber;[53] d) DFT simulation of V4D4 monomer electron densities. Blue volumes indicate areas of negative charge;[80] e) False color TEM of iCVD pV4D4 on spinel particle supplied by Veronica Augustyn of the Manthiram group at the University of Texas- Austin. Coating highlighted in light purple f) Left: TEM of ACNT coated with PEDOT Right: close up of single nanotube coated with PEDOT with schematic overlay of nanotube and volumetric charge storage within PEDOT.[46] a) Reproduced with permission.[58] Copyright 2015, American Chemical Society. b) Reproduced with permission.[64] Copyright 2015, American Chemical Society. c) Reproduced with permission.[53] Copyright 2015, Royal Society of Chemistry. d) Reproduced with permission.[80] Copyright 2015, American Chemical Society. f) Reproduced with permission.[46] Copyright 2014, Wiley-VCH.

3.2.1. Macroscale Devices

In macroscale devices, lithium conduction from the anode to the cathode occurs via a liquid electrolyte. A porous polymer separator, such as polyethylene (PE), between the anode anode and cathode serves to prevent short circuits which cause thermal runaway. However, poor electrolyte solvent wettability and shrinkage at higher temperatures can impede device performance and be a safety hazard respectively. Im and co-workers used iCVD to deposit poly(hexavinyldisiloxane) (pHVDS) on PE separators to address these two issues.[64] Using iCVD for this process allows for the conformal coverage of PE fibers in the separator thus maintaining the pore structure, albeit at a lower pore size. Using the same deposition conditions, a 40-minute growth time was optimal for reducing separator shrinkage, as see in Figure 3b. Also seen in Figure 3b is the same pHVDS film on the separators results in a 30° decrease in the water contact angle, resulting in much better solvent wettability. Finally, the pHVDS films were shown to be electrochemically stable after 70 cycles by no change in the before and after FTIR and XPS spectra.

Another area of interest is the development of new cathode materials to replace $LiCoO_2$, the industrial standard. New materials, such as layered lithium-rich manganese oxides (LLO) offer higher capacities but suffer from capacity loss due to side reactions with the electrolyte. Using conductive polymer coatings on LLO particles can slow these reactions and offer higher capacity retention rates. Recently, Liu et al. demonstrated that ultrathin and conformal oCVD PEDOT coatings on LLO improve their cycling stability.[81] Composite electrodes of 1.12 wt% oCVD PEDOT enabled a much greater capacity retention rate of 91.39% after 50 cycles compared to 71.19% retention rate of pristine LLO. The superior capacity retention rate is attributed to the ultrathin and uniform nature of the PEDOT film on all of the LLO particles.

3.2.2. Microscale Devices

Three dimensional electrode architectures, such as nanowire arrays, allow for higher energy and power densities within a smaller areal footprint. The complexity of the electrode structure necessitates conformal coatings of ultrathin solid polymer electrolyte (SPE) layers, which serve both as a separator and electrolyte. iCVD-synthesized polymers are able to conformally coat high-aspect-ratio structures, as seen in Figure 1b. Gleason and co-workers first reported the use of pV4D4 doped with lithium ions as a room temperature SPE.[36] As deposited 25 nm pV4D4 was shown to be an electrical insulator with electron conductivities $\approx 10^{-11}$ S cm^{-1} and withstand electric fields greater than 10^4 V cm^{-1}, all characteristics essential for the role of electrode separator. pV4D4 doped with lithium perchlorate exhibits room temperature ionic conductivities of $\approx 10^{-8}$ S cm^{-1}, which is similar to solution processed poly(ethylene oxide), the current state of the art. However, the iCVD pV4D4 films have the benefit of being substantially thinner than conventional solution processed films which results in six orders of magnitude lower ionic diffusion time. Rolison and co-workers compared the electropolymerization

(EP) and iCVD synthesis of pV3D3, an analogue of pV4D4 with a smaller ring structure.[53] In this study, 30–50 nm thick pV3D3-synthesized through both routes was deposited on carbon coated silica (C@SiO$_2$) fiber paper. The underlying fiber structure was best retained with the iCVD method, as seen in the SEM cross section in Figure 3c. FTIR analysis of the polymers show that many more vinyl bonds have reacted in the iCVD synthesis compared to the EP synthesis. Correspondingly, the impedance of iCVD pV3D3 is ≈ 60 Ω greater than EP pV3D3, showing it is a better electrical insulator. The iCVD synthesis and deposition kinetics of cyclic polysilazanes (CPSNs), pV3N3 and pV4N4, were studied by Chen et al. as potential SPEs.[82] The poor vinyl bond reactivity of CPSNs results in a much lower degree of crosslinking when compared to their cyclic polysiloxane (CPSO) counterparts, as evidenced by a 10–20° increase in water contact angle hysteresis over CPSOs. A corresponding study by Reeja-Jayan et al. showed that CPSOs have higher ionic conductivities than CPSNs.[80] Moreover, a larger ring structure can lead to an order of magnitude increase in ionic conductivity. Inductively coupled plasma- mass spectroscopy determined that pV4D4 uptakes more lithium ions during the doping process than pV3D3. Density functional theory (DFT) calculations show that pV4D4 has a 9.7 kJ mol^{-1} lower activation energy for lithium uptake compared in pV3D3. DFT simulations also determined that lithium ions reside in areas of negative charge around a V4D4 molecule, as shown in Figure 3d. Gleason and co-workers are currently studying the integration of doped pV4D4 films into full battery architectures. Figure 3e shows a previously unpublished TEM micrograph of iCVD pV4D4 conformally coating a lithium manganese nickel oxide (LMNO) particle, a spinel cathode material. A clear transition from LMNO to pV4D4 is evidenced by the abrupt end of crystalline lattice fringes into an amorphous layer.

3.3. Supercapacitors

Supercapacitors are of interest as another energy-storage device owing to their higher power density and cycle life when compared to batteries. In these devices, both electrodes are immersed in a liquid electrolyte with a porous separator between the two electrodes. Charging the electrodes results in an electric double layer, where capacitance increases with electrode surface area. For this reason, high-surface-area carbon materials, such as nanoporous structures or aligned carbon nanotubes (ACNTs) have been investigated as potential electrodes. The overall capacitance of these devices can be increased via conductive polymer (CP) coatings on the electrode surface. Instead of confining charges only to the surface of carbon allotrope electrodes, they can also be stored throughout the volume of the CP as seen in Figure 3f, thus increasing the pseudocapacitance of the device.[47] Given the need for excellent conformal coverage of architectures at the sub-micrometer or even nanoscale level, a vapor-based polymerization method is ideal for coatings of CP. Two oxidative step polymerization techniques, vapor phase polymerization (VPP) and oCVD, have been used to generate CP coatings.

3.3.1. VPP-Enabled Supercapacitors

In VPP, the substrate of interest is soaked in an oxidant solution and dried. The oxidant impregnated substrate is then placed in a heated chamber where monomer vapors are introduced and polymerization starts. Lee et al. demonstrated the use of solvent co-vapors to tune the capacitance of Ppy coated devices.[49] A highest capacitance of 57.2/g was observed when water was the co-vapor. Jang and co-workers reported the use of Ppy coatings on Co(OH)$_2$ nanostructures in an asymmetric supercapacitor.[50] The device had a voltage window and power density of 1.6 V and 0.53 kW L^{-1} respectively. 89% of capacitance was retained after 5000 cycles.
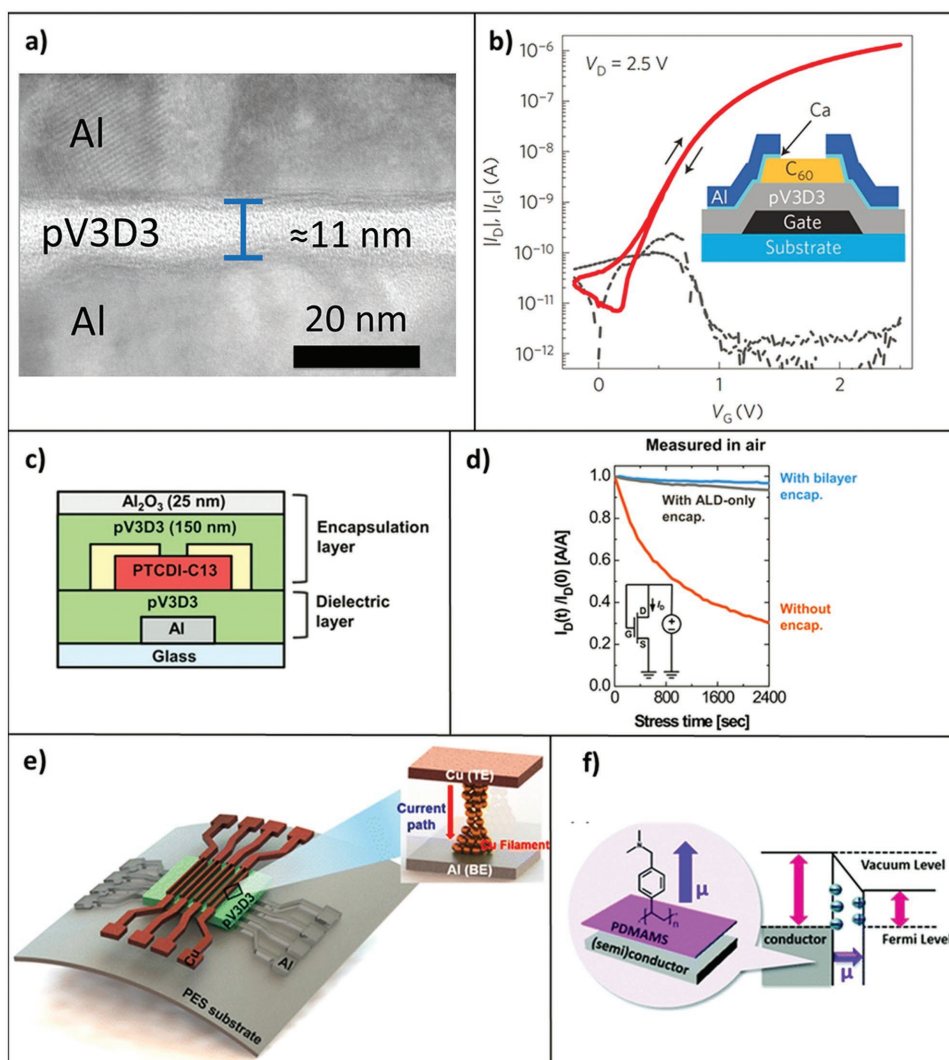
3.3.2. oCVD-Enabled Supercapacitors

Unlike VDP, oCVD is a one step process where monomer and oxidant vapors are simultaneously introduced in the chamber to form a CP film. Lau and co-workers reported the use of ultrathin PTh on porous nanostructures activated carbon enabled increases of 250% in volumetric capacitance with only 10% decrease over 5000 cycles.[52] Wardle, Gleason, and co-workers have investigated PEDOT coated ACNTs composites as negative electrodes for supercapacitors. Vaddiraju et al. first demonstrated conformal coatings of oCVD PEDOT on ACNTs (PEDOT-ACNTs).[45] A 10× volumetric capacity increase over uncoated ACNTs was shown with PEDOT-ACNTs.[46] Asymmetric supercapacitors with PEDOT-ACNT negative electrodes have been created with both ultrahigh density ACNTs[48] and ultrahigh density aligned activated graphene flakes[47] positive electrode with both systems boasting a wide 4 V electrochemical window. The use of graphene flakes as the positive electrode yielded a power density of 149 kW L^{-1} and 89% of capacitance retained over 1000 cycles.[47] The device with an ACNT-based positive electrode had a lower power density of 130.6 kW L^{-1} but a greater capacitance retention of 91% after 5000 cycles.[48] A recent review of asymmetric supercapacitors found that the PEDOT-ACNT system has the best electrochemical performance out of all polymer-based systems.[83]

4. Organic and Hybrid Electronic Devices

"Soft" electronics rely on the mechanical flexibility of the materials involved. oCVD conductive and semi-conductive materials have demonstrated their potential in these flexible organic electronic devices. Flexible insulating layers are also essential components required to work with unconventional substrates and semi-conductors. To this end, polymeric films providing high capacitance, low leakage, high breakdown field and resistance to electrical stresses have been investigated as new insulating layers for organic devices, as well as for fabricating hybrid structures. Owing to the advantageous characteristics of the iCVD process, including the non-destructive nature, conformal surface growth and precise thickness control, they have been integrated into the flexible electronics mainly as, but not limited to, dielectrics and encapsulation barrier layers.

Im et al. first tested iCVD pV3D3 films (with a dielectric constant of 2.2) in a metal/insulator/metal structure (**Figure 4**a).[17] The films exhibited excellent insulating properties with low tunneling-limited leakage characteristics. This was attributed to the low defect density of the pV3D3 films, which was resulted from iCVD's solvent-free nature eliminated the potential for any solvent residues. iCVD's ability to fabricate ultrathin layers, down to sub-10 nm of pinhole-free and uniform thinness, allows high capacitance density of the insulating layers to be achieved. Thus the iCVD pV3D3 films were proposed as high-capacitance gate dielectric for field-effect transistors (FETs). Subsequently in this work, iCVD pV3D3 was grown on a plastic substrate and a variety of channel layers as gate dielectrics to yield flexible FETs (e.g., Figure 4b inset). The devices exhibit ideal, hysteresis-free transfer characteristics and consistently low gate leakage current, as shown in Figure 4b. Following up the pV3D3 homopolymer work, Im and co-workers have further modified the pV3D3 thin film by surface treatment.[55] Oxygen plasma treatment were used to form a molecular-thin oxide capping layer, onto which self-assembly monolayers (SAMs) were tethered by applying silane-based reagents. The capping layer enhances the thermal stability of the dielectrics and provides reactive sites for subsequent silanization. The SAM improves the interface between the dielectric and the pentacene channel layer. As a result, the thin-film transistors (TFTs) with SAM-treated pV3D3 gate dielectric, exhibited substantially higher field-effect mobility and on–off ratio. Recently, the library of iCVD dielectrics was extended to three new polymers: pEGDMA, pIBA, and pPFDA.[60] All exhibited low leakage currents under the condition of being flexed, and were demonstrated as gate dielectric layers for hysteresis-free, low-voltage TFTs. In addition to being used as gate dielectrics, iCVD pV3D3 has also been explored as an encapsulation layer by itself or in conjunction with other materials, due to its long-term stability as well as aforementioned mechanical flexibility and electrical insulation properties. iCVD pV3D3 was first demonstrated to be suitable for use in electrically insulating neural recording array.[84] Its high electrical resistivity allows films as thin as 5 μm to serve as electrical insulation layer for this application. Moreover, it displayed resistance to hydrolysis at elevated temperature and a variety of solvents. In addition, the electrical properties of pV3D3 films exhibit long-term stability over 2.5 years under simulated implant conditions. Having shown its potential as biopassivation layer, iCVD films were further hybridized with inorganic thin films synthesized via PECVD, ALD, and HWCVD to produce barrier layers to vapor transmission.[54,65,85,86] The hybrid films have the advantages of both inorganic and organic films, displaying low vapor transmission and good mechanical flexibility. Coclite et al. synthesized a type of hybrid film by combining PECVD and iCVD in a single-chamber process.[65] The same precursor, HVDSO, was used to produce a multilayer stack composed of SiO$_x$-like layer via PECVD and pHVDSO layer via iCVD. The hybridization was achieved by alternating the polymerization mechanisms. Water vapor transmission rates (WVTRs) of 0.01 g m^{-2} per day at 28 °C, 98% RH were obtained, which represents a barrier improvement factor of 100 over the single SiO$_x$-like layer. iCVD pV4D4 has also been hybridized with Al$_2$O$_3$ deposited by ALD for encapsulation of organic electronic

ADVANCED
SCIENCE NEWS
www.advancedsciencenews.com

ADVANCED
MATERIALS
www.advmat.de

PROGRESS REPORT

Figure 4. Examples of iCVD layers as dielectric and encapsulation layers. a) Cross-sectional TEM of an ultrathin (11 nm) iCVD pV3D3 dielectric layer between two aluminum electrodes forming a MIM device.[17] b) Schematic of a bottom-gated C_{60} FETs with 15.3 nm pV3D3 gate insulators, and its $|I_D|$ versus V_G (solid lines) and $|I_G|$ versus V_G (dotted lines) characteristics. The $|I_D|$ (drain current) exhibits a hysteresis-free transfer characteristic, and the $|I_G|$ (gate leakage current) is consistently low.[17] c) Schematic of a TFTs fabricated with both a iCVD gate dielectric layer (sub-30 nm) and a bilayer encapsulation consisting of iCVD pV3D3 (150 nm)/ALD Al_2O_3 (25 nm).[91] d) The bias-stress induced I_D of PTCDI-C13 TFTs without encapsulation (orange), with ALD Al_2O_3 encapsulation layer (25 nm) only (grey) and with the bilayer encapsulation (i.e., the device configuration in c, blue) as a function of stress time measured in ambient air ($V_G = V_D$ = 15 V).[91] e) Schematic illustration of the iCVD pV3D3-RRAM and its operating mechanism through Cu filament.[92] f) Schematic illustration of the WF changing mechanism due to the dipole moment formed by the PDMAMS modification.[66] a,b) Reproduced with permission.[17] Copyright 2015, Nature Publishing Group. c,d) Reproduced with permission.[91] Copyright 2016, Wiley-VCH. e) Reproduced with permission.[92] Copyright 2016, American Chemical Society. f) Reproduced with permission.[66] Copyright 2016, The Royal Society of Chemistry.

devices.[85] The WVTR of the hybrid encapsulation layer was as low as 2.17×10^{-4} g m^{-2} per day at 38 °C, 90% RH. Currently, the state-of-the-art value of WVTR, 10^{-6} g m^{-2} per day, has been achieved by several methods and materials, such as plasma-enhanced CVD (PECVD)-deposited SiO_2,[87] PECVD-deposited SiN_x/SiO_x multilayer with a polymer overcoat,[88] atomic layer deposition (ALD)-deposited SnO_x,[89] hot-wire CVD (HWCVD)-deposited SiN_x/polymer hybrid multilayer.[90] This state-of-the-art value is also the requirement of new-generation organic electronic devices.[65] Since iCVD polymers have shown great potential in enhancing the WVTR of the inorganic barriers as aforementioned, even lower WVTR may be potentially

achieve in the future. A recent work, interestingly, integrated a layer of pPFDMA onto the outermost of a pV4D4-Al_2O_3 hybrid layer, adding a self-cleaning functionality to the encapsulation layer.[54] At the device level, Im et al. recently demonstrated an organic TFT with iCVD pV3D3 gate dielectric and pV3D3-Al_2O_3 hybrid bilayer encapsulation, as shown in Figure 4c.[91] The device shows a substantially improved source–drain current under 15 V of gate-source voltage as a constant voltage stress in ambient air (Figure 4d). The authors further demonstrated an encapsulated complementary inverter, which exhibited stable, hysteresis-free voltage transfer characteristics (VTC) curves in ambient air even after 22 days.

pV3D3 films were also demonstrated as switching medium in filament-type resistive random access memory (RRAM), owing to its excellent insulating properties and ability to withstand the conditions required for metal filament formation (Figure 4e).[92] The excellent chemical stability of pV3D3 allows RRAM arrays with Al (bottom electrode)/pV3D3/Cu (top electrode) configuration to be fabricated by conventional photolithography. The pV3D3-based RRAM demonstrated unipolar resistive switching (URS) with high on/off ratio (>107), good retention of the on/off ratio (>105 s), excellent cycling endurance (105 cycles), and robust mechanical flexibility. The switching mechanism was attributed to the reversible formation and rupture of Cu filament. It is advantageous over current solution-based polymer RRAMs in uniformity, electrical stability, and long-term stability. This work demonstrates a good way to fabricate a polymer-based, flexible RRAM, which can be used for Internet of Things (IoT) as stated by the authors.

iCVD thin films have extended its application to modify the work function (WF) of electrode (Figure 4f).[66] Ultrathin pDMAMS, a strong electron-donating polymer, deposited onto the electrodes via iCVD effectively reduces its WF by forming an interfacial dipole between the pDMAMS layer and the conductor materials. Gold surfaces modified with ultrathin pDMAMS were used as S/D electrodes of bottom-contact C60 TFTs. The device with and without pDMAMS modification exhibited saturation electron mobility of 0.89 and 0 cm^2 V^{-1} s^{-1} respectively. The authors further showed that pDMAMS layer can be used to n-dope graphene, and from it a n-type graphene TFT can be fabricated. By combining the n-type graphene TFT and a p-type graphene TFT in series, a graphene inverter was demonstrated.

5. Photonic Devices

Photonic devices manipulate light for a variety of applications from smart windows to solar cells. Integrating conducting or semiconducting polymers into these devices are of great interest due to their flexibility and low cost. CVD electronic polymers enable the fabrication of nanomaterials that combine the aforementioned properties with high efficiency and high stability. These polymer films have been used both in electrochromic devices and photovoltaics
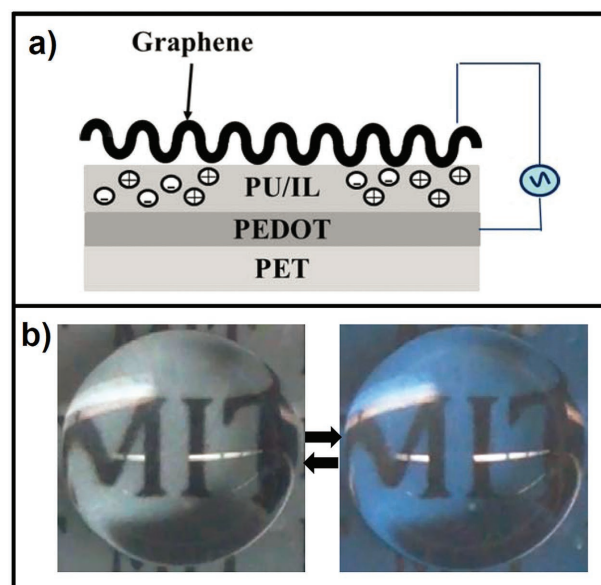
5.1. Electrochromic Devices

Electrochromism, a reversible change in a material's optical properties under an applied voltage, has been extensively studied for applications in smart windows, displays, and antiglare windows.[93] Conjugated polymers can undergo reversible oxidation and reduction, allowing them to change between insulating and conducting forms. This change in their redox state is complemented by a change in their absorption characteristics, making them great candidate as electrochromic materials.[94–96] PEDOT has become the most useful of the commercially-available electrochromic polymers because of its combination of optical properties, stability, and processability.[94]

Ultrathin pinhole-free CVD polymers along with few nanometer thick graphene sheets enable fabrication of devices with enhanced functionality during operation and also flexing conditions. For example, Howden et al. have shown that for deposition on graphene, the CVD PEDOT was pinhole free, while PEDOT:PSS display pinhole defect visible to the human eye. One of the devices with increasing demand is electrochromic devices. In addition, there has been an increasing demand in developing superhydrophobic self-cleaning surfaces.[9,16] Graphene as transparent and conductive ultrathin films have been recently crumpled into self-organized hierarchical structures resembling superhydrophobic leaves.[97–99] Sojoudi and co-workers have recently utilized a novel mechanical self-assembly approach to develop superhydrophobic flexible/stretchable electrochromic devices.[100] They integrated multilayer crumpled graphene as superhydrophobic, transparent, and conductive top electrode with transparent polyurethane (PU) elastomer containing ionic liquid (IL) as dielectric, and oCVD PEDOT as electrochromic bottom electrode in their novel structures (**Figure 5**a). A water droplet stays in Cassie–Baxter state, when the electrochromic nature is observed by applying 10 V AC to the device (Figure 5b).

5.2. Photovoltaics

The demand for more efficient and eco-friendly energy conversion processes is growing rapidly, especially in response to global warming and natural resource depletion. Hence, the development and commercialization of high-performance solar energy conversion systems, which can end the current carbon economy era and thus initiate the solar economy, are of paramount importance in both academia and industry.[101–105] In this regard, solar cells have offered great promise due to their

Figure 5. a) Schematic of superhydrophobic flexible electrochromic devices made of crumpled graphene and oCVD PEDOT as electrodes. b) A clear reversible transition from transparent to blue color obtained by applying 10 V AC to the device.[100]

**ADVANCED
SCIENCE NEWS**

www.advancedsciencenews.com

**ADVANCED
MATERIALS**

www.advmat.de

PROGRESS REPORT

potential to enable a clean, sustainable, and cost-effective solar energy conversion from photons to electricity.

However, improvements in the efficiency, stability, and economics of photovoltaic technologies are needed to achieve commercialization worldwide. To address these challenges, inexpensive organic photovoltaics (OPVs) which can be manufactured by cost effective roll-to-roll processes have been proposed.[20] In the Gleason lab, a variety of polymer thin films have been developed for integration into to OPVs via oCVD and iCVD. The polymer thin films synthesized by oCVD and iCVD have played key roles in the devices serving as hole transporting layers (HTL),[19] electron transporting layers (ETL),[66] polymeric electrolyte,[67,69,106] and organic encapsulation preventing O_2 and moisture permeation.[85,107]

5.2.1. oCVD-Based Devices

oCVD, as previously described, enables the formation various insoluble semiconducting and conducting conjugated polymer thin films, which are very difficult to process by typical solution-based methods. The oCVD process operates at moderate vacuum (≈0.1 Torr) and low temperature (25–150 °C).[20] This technique continues to be optimized for poly(dioxythiophene)

(PEDOT), the most promising candidate to date for a polymeric transparent and flexible electrodes for OPV.[23] Improvement in PEDOT properties have been explored through variation in the choice oxidant and in pulsing of the delivery of the monomer, a method termed oxidative Molecular Layer Deposition (OMLD).[108] The mechanism of electronic conduction and its temperature dependence in oCVD PEDOT was quantitatively modeled using a cross-grain approach.[109] This model predicts that when film thicknesses are on the order of dimension of a PEDOT crystallite with in the film, the electrical conductivity becomes two dimensional (2D). The faster lateral diffusivity of the 2D mechanism explains why thin PEDOT films are often more conductive than identical films which are simply thicker.

Recently, neutral polymeric hole transporting layers (HTLs) have been devised by Jo et al.[19] by integrating patterned Cl⁻-doped poly(3,4-dimethoxythiophene) (PDMT) thin films into organic photovoltaic devices (OPVs) using a conventional single-bilayer-heterojunction architecture as shown in **Figure 6**a. Using this device architecture, a wide range of thicknesses of PEDOT:PSS and PDMT HTLs were compared. Figure 6b demonstrates that the oCVD PDMT HTL enhances device stability by allowing 83% of the initial PCE (4.1%) to be retained after 17 days of storage in a N_2 glovebox. In contrast,
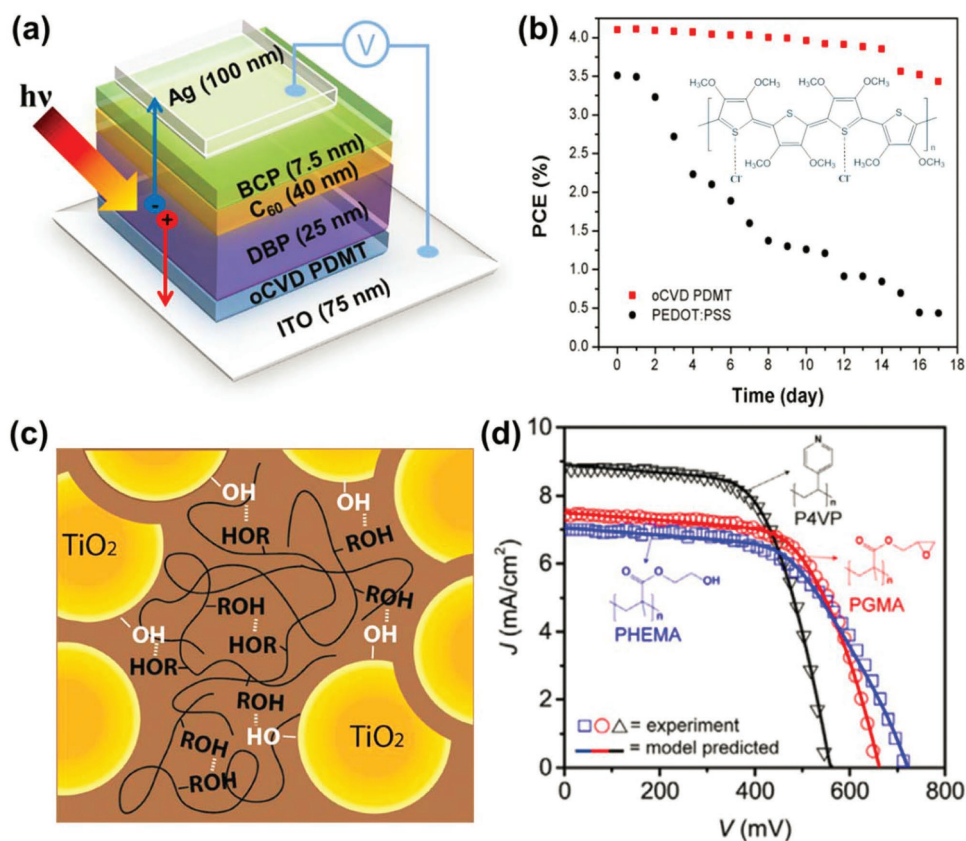
Figure 6. a) Device architecture scheme of DBP/C_{60} solar cells with oCVD-processed poly(3,4-dimethoxythiophen) (PDMT) HTLs;[19] b) PCE evolution of devices with respect to storage time under N_2 atmosphere, and 2D molecular structure of quinoid-form Cl⁻-doped PDMT;[19] c) Schematic illustration of strong hydrogen bonding among hydroxyl groups on TiO₂ surface, PGL hydroxyl groups, and PGL ether groups;[69] d) Modelled (solid) and experimental (symbol) current–voltage curves of polymer-electrolyte DSSCs.[106] a) reproduced with permission.[19] Copyright 2016, Wiley-VCH. c) reproduced with permission.[69] Copyright 2015, Wiley-VCH. d) reproduced with permission.[106] Copyright 2015, Elsevier.

the conventional PEDOT:PSS HTL retains only 12% of its initial PCE (3.5%).

5.2.2. iCVD-Based Devices

The iCVD method can be used to create polymeric electrolytes, thus lending this technique to the fabrication gel nanocomposites for use in devices like dye sensitized solar cells (DSSCs). A network made of nanoparticles affords provides a large surface area for energy harvesting devices. However, solution-based methods to infiltrate the network with gel-polymer electrolytes often results in reduced nanoparticle loading. To increase nanoparticle loading, Hsieh et al. have demonstrated that polyglycidol (pGL) is able to be uniformly grown on mesoporous layers of TiO_2 nanoparticle networks (TNN) using iCVD.[69] Unlike the typical free radical polymerizations used by iCVD, a cationic ring opening polymerization of PGL has been enabled by using boron-trifluoride-based initiators. A conformal PGL coating attained 91% pore space filling through the cationic ring opening polymerization. This enables pGL nanocomposites with high TiO_2-nanoparticle loading of 82 wt% and a corresponding glass transition temperature (T_g) increase by 50–60 °C compared to the bulk PGL polymer. As Figure 6c illustrates, the large T_g increase is attributed to strong hydrogen bonding interactions among hydroxyl groups on TiO_2 surface, pGL hydroxyl groups, and pGL ether groups. These strong interactions enable polymer nanocomposites with high nanoparticle loading which is necessary for high-performance energy devices.

iCVD synthesis of other polymer electrolyte chemistries for DSSCs have also been studied. Janakiraman et al. have investigated the reaction kinetics of poly(vinylpyrrolidone) (pVP) and poly(4-vinylpyridine) (p4VP) synthesis via iCVD, by using Fourier transform infrared spectroscopy, X-ray photoelectron spectroscopy and gel permeation chromatography.[67] Based on the outcomes from the previous research, Smolin et al. has completed the application of iCVD-processed poly(2-hydroxyethyl methacrylate) (pHEMA), poly(glycidyl meth-acrylate) (pGMA), and p4VP to DSSCs as polymeric electrolytes.[106] As the data in Figure 6d show, each polymer's performance as electrolyte in DSSCs has been studied theoretically and experimentally. 1D first-principles macroscopic DSSC mathematical modelling has verified that the polymer's pendant groups greatly impacts the conduction band position of TiO_2, the back electron transfer at. Calculations show the difference between the conduction band and the electrolyte redox potential are 1.06, 0.99, and 0.87 eV for pHEMA, pGMA, and p4VP respectively. The estimated recombination rate constants for P4VP and PGMA are 54 and 19% lower than that of PHEMA respectively. Finally, this study confirms that DSSC performance characteristics such as open-circuit voltage (V_{OC}), J_{SC}, and FF can be manipulated by employing different polymer electrolytes.[106]
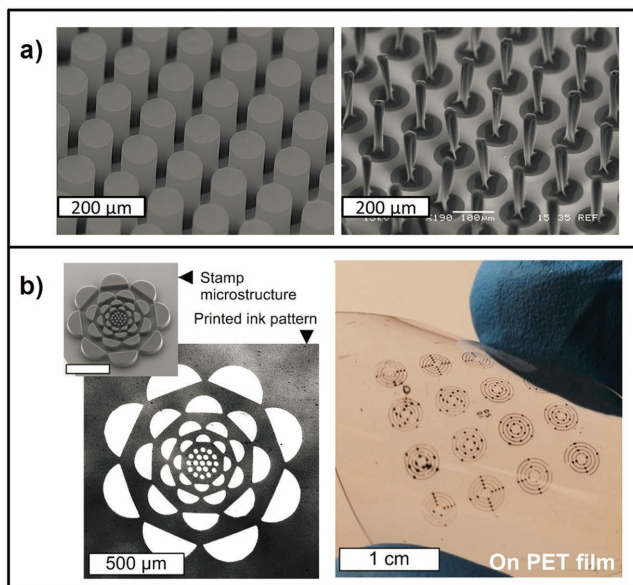
The studies fulfilled by Perrotta et al. and Kim et al. have demonstrated that iCVD polymers can also play a key role as organic encapsulation barriers to prevent O_2 and moisture permeation into organic electronic devices.[85,107] To prove the moisture and O_2 permeation barrier properties of the organic interlayers fabricated by iCVD, both studies have measured water vapor transmission rate (WVTR) by carrying out a calcium test. There is a clear correlation between WVTR and defect density, although the correlation based on calcium test data is not perfectly fit. The smaller defect density and the lower WVTR show that iCVD is an effective surface modification technique to strengthen moisture and O_2 permeation barrier properties.[85,107]

6. Advanced Printing

Porous nanostructures are becoming key features for the fabrication of a wide range of devices for energy generation, storage, and recovery applications, where porosity enables enhanced device performance. Direct-printing of electronic features is attractive due to their rapid rate, material flexibility, and lower cost in equipment and operation. Several well-established methods, including screen, gravure (intaglio), flexographic (relief), and inkjet printing have been adapted to pattern electronic materials with high throughput, yet their resolution (minimum feature size) is limited to ≈20 μm.[110] Flexography in principle may achieve printed features matching the stamp geometry, by loading the liquid ink directly on the upraised stamp structures and relief transfer under contact.[111,112] These direct-printing technologies also leverage advances in functional inks including metallic and semiconductor colloidal solutions which are key to applications including thin-film transistors and transparent electrodes for use in large-area displays, touchscreen devices, and solar panels. Although elastomeric stamps can easily be fabricated with micrometer-scale and smaller features, the liquid transfer between two solid surfaces is prone to liquid spreading, which prevents the transfer of uniform, thin layers for feature sizes smaller than 20–50 μm.[113] Wettability control of such porous nanostructures is needed to fully utilize the high surface area associated in such structures. The conformality of the CVD polymers offers a unique way of controlling the wettability of porous nanomaterials. One of the widely- researched porous nanomaterials is CNTs. The CVD synthesis of vertically aligned CNTs (VA-CNTs)[114] using lithographically-patterned catalyst films directly creates bulk microstructures with tunable electrical and mechanical properties as well as high porosity (>99%).[37,115,116] The large surface area of VA-CNTs with combined control of microscale geometry and nanoscale porosity is beneficial for their applications in batteries[117] and supercapacitors,[118] surface wettability control,[119] and liquid ink direct contact printing.[114] However, as the spacing between the individual CNTs decreases and the resulting aspect ratio increases, the surface area per unit volume also increases significantly. Thus, the VA-CNTs become increasingly influenced by surface forces, such as capillary forces when exposed to liquids. **Figure 7**a shows SEM images of the as-made patterned VA-CNT micropillars (left) and after their wetting and subsequent drying with low-surface-tension dimethoxyethane liquid (right). This aggregation and densification process in nano/micro filaments due to exposure to liquids, also referred to as elastocapillary self-assembly, has been used as a fabrication step to enhance the functionality of CNTs for applications in microelectonics, interconnects, MEMS devices, micro sensors, trapping devices, bioprobes, and energy-storage devices.[120] For example, De Volder et al.

ADVANCED
SCIENCE NEWS
www.advancedsciencenews.com

ADVANCED
MATERIALS
www.advmat.de

PROGRESS REPORT

Figure 7. a) Impact of the conformal pPFDA coating on the wettability of the patterned CNT micropillars. Left panel is the SEM image of the patterned CNT micropillars and right panel is the SEM imaging after wetting of the sample with water and drying. b) Utilizing nanoporous microstructures made of the pPFDA-coated patterned CNTs as stamp for flexoprinting of electronic features on glass and PET substrates. The scale bar shown in the inset is 500 μm.

have demonstrated an enhancement in the mechanical robustness of the CNTs through capillary densification (100-fold enhancment in the Young's modulus) and have developed 3D microstructures as molds for mass production of 3D polymer structures.[121] Despite these advances, elastocapillary densification and shrinkage from surface tension forces applied during liquid infiltration and evaporation,[120] have precluded the application of VA-CNT forest porosity in liquid environments.

Recently, the elastocapillary densification of the CNTs was prevented by conformal deposition of an ultrathin protective layer of poly(perfluorodecylacrylate), poly(1H,1H,2H,2H-perfluorodecylacrylate) (pPFDA), a low surface energy polymer, on the CNTs via iCVD.[122] Uniformity and conformality of the pPFDA deposition via iCVD on the CNT micropillars has been confirmed by the SEM-EDX mapping of the coated CNT micropillars (Figure 7a). Polymer coating via the vapor-based and solvent-less iCVD method has also been studied to form polymeric duplicates of rose petal structures.[123] Lau et al. took a bio-inspired approach to the problem of developing superhydrophobic surfaces using iCVD thorugh mimicking designs found in nature.[119] They enhanced the superhydrophobic effect on CNTs by combining nanoscale roughness of the CNTs with a a hydrophobic poly(tetrafluoroethylene) (PTFE) coating. Ye et al. have demonstrated successful transfer of aligned multi-walled carbon nanotube (MWNTs) after being functionalized with poly(glycidyl methacrylate) (PGMA) via iCVD.[86] They have also shown improved mechanical properties and stability in MWNTs after polymer deposition. In the recent work, Sojoudi et al.[122] have studied the impact of the conformal pPFDA coating on wetting and drying of the VA-CNTs by liquids, which vary significantly in surface tension, using

in-situ microscopy and imaging to examine liquid infiltration and densification processes in the CNT microstructures. Utilizing pPFDA clusters coated crust of entangled CNTs on top of the micropillars, they have formed nanotextured surfaces possessing re-entrant features preventing the penetration of low-surface-tension liquids (e.g., hexadecanethiol, dimethoxyethane, acetone). Sequential environmental SEM images captured during drying of the dimethoxyethane droplet on the pPFDA-coated CNT pillars have indicated prevention of ellastocapillary formation. Small microdroplets form duing the drying process, have shown prevention of evaporation-triggered Cassie to Wenzel transition.

Kim et al. have developed a porous stamp material, which holds the ink within each stamp feature and transfers the ink with high-fidelity via conformal contact to the target substrate, enabling higher resolution direct printing while preserving the scalability and versatility of conventional flexography methods. They have used VA-CNTs as the microstructured nanoporous stamp, conformally coated with the pPFDA via iCVD, combined with multiple plasma treating processes. Along with the scalable manufacturability, the polymer-coated CNT microstructures have provided not only the mechanical compliance required for conformal contact against target substrates (similar to that attained with the solid elastomers) but also the nanoscale porosity required for solution-based electronic materials to be held inside the structures. By further engineering the structures and using appropriate inking steps, the new porous stamps have enabled printing ultrathin layers of ink material onto target substrates via nanoscale liquid transfers under microscale conformal contact. Using the engineered CNT stamps, they have shown versatile micro patterns of electronic materials, with feature sizes on the scale of a few micrometers, which can be directly printed on both rigid and compliant surfaces (Figure 7b).

7. Patterning

The successful integration of functional polymeric films into devices requires patterning features into these organic thin films. The substrates which underlie patterned films include non-planar, planar, porous, and membrane structures with varying degrees of roughness. A major benefit of vapor phase processing is conformality, a concept which refers to the ability to produce coatings of uniform thickness on all surfaces of geometric complex substrate. Additionally, the substrates can be comprised of either soft or hard materials and ranging from very hydrophilic to extremely hydrophobic. Because effects, such as dewetting, can be eliminated, a single CVD polymerization processes can be compatible with multiple substrate types which vary substantially in their surface energies. This section addresses the recent approaches and the abilities of polymer CVD for patterning as summarized in **Table 2**.

Perhaps the simplest method to generate patterns is masking substrates during the deposition is using a physical mask. Barr et al. successfully fabricated oCVD PEDOT features tens of micrometers in size on glass, paper, and plastic substrates with a metal shadow mask. The resulting PEDOT patterns served as a transparent conductive anode for thin organic

Table 2. Vapor-phase-deposited polymers for patterning.

Approach	Key element	CVD	Polymer[a]	Substrate	Resolution[b]	Ref.
Masking	Metal shadow mask	oCVD	PEDOT	Paper, Plastic films	<1 cm	[38,117]
	Micro-stencil	Pyrolysis	PPXPF-co-PX	Thermoplastics	≈150 µm	[73]
	Photomask	iCVD	P(Vcin-co-NIPAAm), P4VP, PoNBMA	Si, Glass rods	10–50 µm	[74,124]
		MLD[c]	Polyurea	Si	4 µm	[71,125]
E-beam	No crosslinking	MLD	Polyurea	Si	<50 nm	[126]
Pre-patterns	Transition metals	iCVD	P4VP, PPFDA, PoNBMA, PPFM	Si, Paper	<1 cm	[61–63]
Inhibitor	Metals + electrical charge	Pyrolysis	Parylene	Metal	<100 µm	[70]
	SAM[d]	Pyrolysis	Parylene	Si, Au	≈3 µm	[30]
Oxidant	DPN[e]	VPP	PEDOT	Si, Au	250 nm	[127]
	Inkjet	VPP	PEDOT	Glass, Plastic films	80–100 µm	[128]
DSA[f]	Topcoat	iCVD	PDVB[g]	Si	<10 nm	[41]

[a]Polymer name abbreviations. P(PXPF-co-PX): poly(p-xylylene-4-carboxylic acid pentafluorophenolester-co-xylylene); P(Vcin-co-NIPPAm): poly(vinylcinnamate); P4VP: poly(4-vinyl pyridine); PoNBMA: poly(ortho-nitrobenzyl methacrylate); PPFDA: poly(1H,1H,2H,2H-perfluorodecyl acrylate); PPFM: poly(pentafluorophenyl methacrylate); [b]Highest resolution shown in the literature; [c]MLD: Molecular layer deposition; [d]SAM: self-assembled monolayer; [e]DPN: dip-pen lithography; [f]DSA: directed self-assembly; [g]PDVB: poly(divinylbenzene)

photovoltaics.[38,117] oCVD can generate higher resolution patterns than VPP that relies on the solvent casting of oxidants because oCVD delivers both of oxidant and EDOT vapors.[38] Micro-stencils made from the elastomeric material poly(dimethylsiloxane) (PDMS) created bio-functional square patterns of pyrolysis generated polycyclophane with ≈150 µm size on a thermoplastic substrate enabling the good sealing between the mask and substrate.[73]

To achieve higher resolution features, photolithography using an optical mask becomes the most reliable process to achieve fine patterns in the semiconductor industry. One of the current challenges is to shrink feature sizes down to sub-10 nm in a cost-effective way. Therefore, development of highly sensitive, chemically homogeneous, and ultrathin photoresist films has been of interest. Zhou et al. demonstrated ultrathin polyurea resist films deposited by molecular layer deposition (MLD) for the first time.[71,125] The self-limiting nature of MLD enabled the control of the thickness, stoichiometric compositions, and placement of functional moieties. MLD exactly placed photoacid generator (PAG), a chemical amplifier, within the MLD polyurea films allowing the uniform distribution of PAG within photoresist films thick of sub-10 nm. In a separate work, a highly sensitive e-beam resist was developed by polyurea films with MLD for sub-50 nm patterning.[126] The elimination of the aromatic components in the MLD films prevents the 30 nm thick polyurea films from cross-linking under e-beam exposure, thereby producing higher resolution patterns (≈40 nm) with sub-100 C cm^{-2} exposure. Petruczok et al. reported that iCVD achieved the Cr/Au patterns on curved substrates with the combination of iCVD poly(4-vinyl pyridine) and post-soaking the films with a photoactive molecule.[124] For this geometry of substrate, the traditional method of applying resist to by spin coating would be challenging. In further work, UV-light-responsive poly(vinyl cinnamate) was iCVD copolymerized with temperature responsive poly(N-isopropyl acrylamide) for reversible patterning.[74]

Yet another strategy is using pre-patterns of an inhibitor or oxidant prior to the deposition.[30,61–63,70,127,128] The pre-patterns of transition metal (or salts) delayed the film growth selectively in iCVD, while pre-patterns of Fe (III) tosylate Fe(Tos)$_3$ composites, as an oxidant, promoted the deposition in VPP. The Gupta group published a series of papers on selective iCVD with the pre-patterns of transition metal salts such as CuCl$_2$ and Cu(NO$_3$)$_2$.[61–63] They formed the pre-patterns by spin-casting or spay-coating with transition salt solutions before iCVD. They investigated some combinations of several transition metal salts and polymers to evaluate the inhibition effect and observed that metal cations affect the ability to inhibit the polymer deposition.[63] This approach enabled the selective deposition of fluoropolymers on porous structures such as papers. They further demonstrated a paper-based microfluidic device with the patterned fluoropolymer barriers. The barriers allowed the containment of organic solvents within the paper-based device so that it can detect water insoluble analytes in the solvents.[62] For the inhibition effect of transition metal salts, they examined the changes in the oxidation state of metals during the iCVD process and concluded that the salts quenched the propagating radicals which led a reduction of the oxidation states of the metal.[61] In addition to such transition metal composites, it was recently reported that applying the electrical charge to metals can inhibit the growth of PPX films via VPP and enhance the inhibition effect, irrespective of the substituted functionality.[70] Wu and co-workers effectively inhibited the deposition of parylene C and aldehyde-functionalized PPX on metal substrates supplying an electrical charge, while the growth inhibition of both films failed with no electrical charge. They explained that supplying electrical energy to the substrate increases the transition of the surface energy, thus reducing the sticking coefficient by one order of magnitude for a substrate: for example, iron.[70] Micropatterned self-assembled monolayers (SAMs) on a gold substrate by microcontact printing (µCP) can also inhibit the growth of functional paracyclophane films.[30] Gall et al. demonstrated that the different chain groups of SAMs have

different abilities to inhibit the film growth; CH$_3$-terminated SAMs inhibited effectively, while COOH- and OH- terminated SAMs did not.[30] In contrast, the pre-patterns of oxidants can encourage the selective growth of PEDOT films by VPP. Two techniques contributed to printing the oxidant inks: dip-pen lithography (DPN) and inkjet printing.[127,128] In both techniques patterned oxidant inks with unique compositions were formed on substrates prior to introducing vapors of monomer. The key for successful selective deposition of PEDOT via the techniques is unique oxidant inks compatible to each printing technique. O'Connell et al. mixed Fe(Tos)$_3$ oxidant with an amphiphilic block copolymer to control the water content, which is critical to transfer the oxidant ink to substrates from the tip of atomic force microscopy (AFM) in DPN as well as to stabilize the printed ink on the substrate during the polymerization.[127] They successfully shrunk the PEDOT pattern size down to 250 nm in width. For inkjet printing, localized oxidant inks formulated with triblock copolymers deliver good flow characteristics and stability.[128] The resulting PEDOT patterns achieved the high conductivity ($\approx$1000 S cm^{-1}) and were successfully built in organic electrochemical transistors as an electrode.

Recently, Kim et al. presented a unique way to use iCVD polymer for sub-10 nm patterning in conjunction with directed self-assembly (DSA).[41] They deposited ultrathin iCVD polymer films on a highly segregating (high χ) block copolymer (BCP) film as a topcoat. As a result, the iCVD topcoat created sub-10 nm patterns from chemical guide strips of DSA after the thermal anneal. Their spectroscopic studies revealed that iCVD formed the unique interface between the BCP and topcoat, which is a mixed interfaced made by grafting and intermolecular entanglements. This unusual interface is not observed in a spun-cast topcoat.

For patterning, the CVD polymers have advantages over conventional liquid-based polymerizations in; scalability, uniformity, tunability, and the option to select from a wide selection of substrate materials. Key areas for continued research on the selective deposition of CVD polymers are determining the detailed mechanism(s) by which the selective deposition is achieved; determining the range of possibilities for both the substrates and patterned films; enabling the selective patterned of films of $\approx$10 nm or greater thickness; and achieving feature resolution significantly below 1 μm.

8. Conclusion

CVD polymerization is an enabling technology for a wide range of devices including chemical and biological sensors, batteries/supercapacitors, photovoltaics, and novel nanostructured devices. The organic layers generated by CVD technology exhibit benefits such as mechanical flexibility, specific and versatile organic functionality, and low-temperature synthesis. The CVD polymer method also enables novel approaches to patterning and advanced printing. A key merit of the CVD polymer approach is often its ability to achieve conformal coating of CVD polymers on a multitude of different structures. In addition, other merits contribute to their own specific applications as well. This review paper demonstrated the advantages of CVD technology in fabricating devices with the applications shown in Figure 1. In chemical/bio-sensing, the added functional groups provide docking sites for various sensing elements, while the modulation of the Fermi level in the oCVD polymers also provides great sensing signals. In the applications of batteries and supercapacitors, the excellent dielectric property of the iCVD polymers and the conformal coating comprised of CVD conducting polymers enhanced the performance prominently. When fabricating photovoltaic devices, the solvent-free neutral feature of oCVD polymer lead to an efficient hole transporting layer. The insulating transparent and water repelling nature of the iCVD polymers facilitated the application of insulation and encapsulation of various devices. Last, but not least, the polymer synthesized via the iCVD technique provides the enormous opportunity for advance printing and sub-10 nm patterning. With all of the applications discussed above, iCVD and oCVD techniques are very versatile and powerful tools in fabricating various devices with insulating or conducting polymers.

[1] K. K. Gleason, *CVD Polymers: Fabrication of Organic Surfaces and Devices*, Wiley-VCH, Weinheim, Germany **2015**.

[2] K. L. Choy, *Prog. Mater. Sci.* **2003**, *48*, 57.

[3] S. Fan, M. G. Chapline, N. R. Franklin, T. W. Tombler, A. M. Cassell, H. Dai, *Science* **1999**, *283*, 512.

[4] A. Reina, X. Jia, J. Ho, D. Nezich, H. Son, V. Bulovic, M. S. Dresselhaus, K. Jing, *Nano Lett.* **2009**, *9*, 30.

[5] N. D. Boscher, M. Wang, A. Perrotta, K. Heinze, M. Creatore, K. K. Gleason, *Adv. Mater.* **2016**, *28*, 7479.

[6] R. Yang, H. Jang, R. Stocker, K. K. Gleason, *Adv. Mater.* **2014**, *26*, 1711.

[7] R. Yang, E. Goktekin, K. K. Gleason, *Langmuir* **2015**, *31*, 11895.

[8] R. Yang, E. Goktekin, M. Wang, K. K. Gleason, *J. Biomater. Sci. Polym. Ed.* **2014**, *25*, 1687.

[9] H. Sojoudi, G. H. McKinley, K. K. Gleason, *Mater. Horiz.* **2015**, *2*, 91.

[10] H. Sojoudi, M. R. Walsh, K. K. Gleason, G. H. McKinley, *Langmuir* **2015**, *31*, 6186.

[11] H. Sojoudi, M. R. Walsh, K. K. Gleason, G. H. McKinley, *Adv. Mater. Interfaces* **2015**, *2*, 1500003.

[12] H. Sojoudi, M. Wang, N. D. Boscher, G. H. McKinley, K. K. Gleason, *Soft Matter* **2016**, *12*, 1938.

[13] A. T. Paxson, J. L. Yagüe, K. K. Gleason, K. K. Varanasi, *Adv. Mater.* **2014**, *26*, 418.

[14] G. Yoo, Y. Yoo, J.-H. Kwon, C. Darpito, S. K. Mishra, K. Pak, M. S. Park, S. G. Im, J.-W. Yang, *Green Chem.* **2014**, *16*, 312.

[15] S. J. P. McInnes, E. J. Szili, S. A. Al-Bataineh, R. B. Vasani, J. J. Xu, M. E. Alf, K. K. Gleason, R. D. Short, N. H. Voelcker, *Langmuir* **2016**, *32*, 301.

[16] N. Chen, D. H. Kim, P. Kovacik, H. Sojoudi, *Annu. Rev. Chem. Biomol. Eng.* **2016**, *7*, 373.

[17] H. Moon, H. Seong, W. C. Shin, W.-T. Park, M. Kim, S. Lee, J. H. Bong, Y.-Y. Noh, B. J. Cho, S. Yoo, S. G. Im, *Nat. Mater.* **2015**, *14*, 628.

[18] X. Wang, A. Ugur, H. Goktas, N. Chen, M. Wang, N. Lachman, E. Kalfon-Cohen, W. Fang, B. L. Wardle, K. K. Gleason, *ACS Sens.* **2016**, *1*, 374.

[19] W. J. Jo, J. T. Nelson, S. Chang, V. Bulović, S. Gradečak, M. S. Strano, K. K. Gleason, *Adv. Mater.* **2016**, *28*, 6399.

[20] A. M. Coclite, R. M. Howden, D. C. Borrelli, C. D. Petruczok, R. Yang, J. L. Yagüe, A. Ugur, N. Chen, S. Lee, W. J. Jo, A. D. Liu, X. X. Wang, K. K. Gleason, J. L. Yague, *Adv. Mater.* **2013**, *25*, 5392.

[21] B. Reeja-Jayan, P. Kovacik, R. Yang, H. Sojoudi, A. Ugur, D. H. Kim, C. D. Petruczok, X. X. Wang, A. D. Liu, K. K. Gleason, *Adv. Mater. Interfaces* **2014**, *1*, 1400117.

[22] K. Chan, K. K. Gleason, *Langmuir* **2005**, *21*, 11773.

[23] D. Bhattacharyya, R. M. Howden, D. C. Borrelli, K. K. Gleason, *J. Polym. Sci., Part B: Polym. Phys.* **2012**, *50*, 1329.

[24] E. Danesh, F. Molina-Lopez, M. Camara, A. Bontempi, A. V. Quintero, D. Teyssieux, L. Thiery, D. Briand, N. F. De Rooij, K. C. Persaud, *Anal. Chem.* **2014**, *86*, 8951.

[25] S. H. Baxamusa, A. Suresh, P. Ehrmann, T. Laurence, J. Hanania, J. Hayes, S. Harley, D. D. Burkey, *Chem. Vap. Deposition* **2015**, *21*, 267.

[26] Y. Mao, K. K. Gleason, *Langmuir* **2004**, *20*, 2484.

[27] X. Deng, S. He, F. Xie, C. Friedmann, H. Hess, J. Lahann, *Adv. Mater.* **2016**, *28*, 2367.

[28] J. Hao, K. C. K. Cheng, L. G. Kruger, L. Larsson, J. V. Sugai, J. Lahann, W. V. Giannobile, *Adv. Mater.* **2016**, *28*, 3145.

[29] L. Shen, K. C. K. Cheng, M. Schroeder, P. Yang, E. N. G. Marsh, J. Lahann, Z. Chen, *Surf. Sci.* **2016**, *648*, 53.

[30] F. B. L. Gall, C. Friedmann, L. Heinke, H. Arslan, C. Azucena, A. Welle, A. M. Ross, C. Woll, J. Lahann, *ACS Nano* **2015**, *9*, 1400.

[31] H. Zhou, S. F. Bent, *J. Vac. Sci. Technol. A* **2013**, *31*.

[32] Y. Takahashi, M. Iijima, Y. Oishi, M. Kakimoto, Y. Imai, *Macromolecules* **1991**, *24*, 3543.

[33] P. Kovacik, S. M. Willis, J. D. Matichak, H. E. Assender, A. A. R. Watt, *Organ. Electron.* **2012**, *13*, 687.

[34] D. B. Chrisey, A. Pique, R. A. McGill, J. S. Horwitz, B. R. Ringeisen, D. M. Bubb, P. K. Wu, *Chem. Rev.* **2003**, *103*, 553.

[35] F. Cicoira, C. Santato, *Organic Electronics: Emerging Concepts and Technologies*, John Wiley & Sons, Hoboken, NJ, USA, **2013**.

[36] N. Chen, B. Reeja-jayan, J. Lau, P. Moni, A. Liu, B. Dunn, K. K. Gleason, *Mater. Horiz.* **2015**, *2*, 309.

[37] N. Chen, P. Kovacik, R. M. Howden, X. X. Wang, S. Lee, K. K. Gleason, *Adv. Energy Mater.* **2015**, *5*, 1401442.

[38] M. C. Barr, J. A. Rowehl, R. R. Lunt, J. Xu, A. Wang, C. M. Boyce, S. G. Im, V. Bulovic, K. K. Gleason, *Adv. Mater.* **2011**, *23*, 3499.

[39] P. Kovacik, G. D. Hierro, W. Livernois, K. K. Gleason, *Mater. Horiz.* **2015**, *2*, 221.

[40] G. Ozaydin-Ince, A. M. Coclite, K. K. Gleason, *Rep. Prog. Phys.* **2012**, *75*, 016501.

[41] D. H. Kim, H. S. Suh, S. Xiong, L. Ocola, P. Nealey, K. Gleason, presented at *2015 American Institute of Chemical Engineeris Annual Meeting*, Salt Lake, UT, USA, November, **2015**.

[42] S. Vaddiraju, K. K. Gleason, *Nanotechnology* **2010**, *21*, 125503.

[43] S. Vaddiraju, K. Seneca, K. K. Gleason, *Adv. Funct. Mater.* **2008**, *18*, 1929.

[44] X. Wang, S. Hou, H. Goktas, P. Kovacik, F. Yaul, A. Paidimarri, N. Ickes, A. Chandrakasan, K. K. Gleason, *ACS Appl. Mater. Interfaces* **2015**, *7*, 16213.

[45] S. Vaddiraju, H. Cebeci, K. K. Gleason, B. L. Wardle, *ACS Appl. Mater. Interfaces* **2009**, *1*, 2565.

[46] N. Lachman, H. Xu, Y. Zhou, M. Ghaffari, M. Lin, D. Bhattacharyya, A. Ugur, K. K. Gleason, Q. M. Zhang, B. L. Wardle, *Adv. Mater. Interfaces* **2014**, *1*, 1400076.

[47] Y. Zhou, N. Lachman, M. Ghaffari, H. Xu, D. Bhattacharya, P. Fattahi, M. R. Abidian, S. Wu, K. K. Gleason, B. L. Wardle, Q. M. Zhang, *J. Mater. Chem. A* **2014**, *2*, 9964.

[48] Y. Zhou, H. P. Xu, N. Lachman, M. Ghaffari, S. Wu, Y. Liu, A. Ugur, K. K. Gleason, B. L. Wardle, Q. M. Zhang, *Nano Energy* **2014**, *9*, 176.

[49] J. E. Lee, Y. Lee, K.-J. Ahn, J. Huh, H. W. Shim, G. Sampath, W. B. Im, Y.-i. Huh, H. Yoon, *Sci. Rep.* **2015**, *5*, 8420.

[50] J. S. Lee, D. H. Shin, W. Kim, J. Jang, *J. Mater. Chem. A* **2016**, *4*, 6603.

[51] N. Alizadeh, A. A. Ataei, S. Pirsa, *J. Iran. Chem. Soc.* **2015**, *12*, 1585.

[52] S. Nejati, T. E. Minford, Y. Y. Smolin, K. K. S. Lau, *ACS Nano* **2014**, *8*, 5413.

[53] M. B. Sassin, J. W. Long, J. M. Wallace, D. R. Rolison, *Mater. Horiz.* **2015**, *2*, 502.

[54] S. Y. Kim, B. J. Kim, D. H. Kim, S. G. Im, *RSC Adv.* **2015**, *5*, 68485.

[55] H. Seong, J. Baek, K. Pak, S. G. Im, *Adv. Funct. Mater.* **2015**, *25*, 4462.

[56] I. Y. Jung, J. B. You, B. R. Choi, J. S. Kim, H. K. Lee, B. Jang, H. S. Jeong, K. Lee, S. G. Im, H. Lee, *Adv. Healthcare Mater.* **2016**, *5*, 2168.

[57] G. Urstöger, R. Resel, G. Koller, A. M. Coclite, G. Urstoger, *J. Appl. Phys.* **2016**, *119*, 135307.

[58] C. Ranacher, R. Resel, P. Moni, B. Cermenek, V. Hacker, A. M. Coclite, *Macromolecules* **2015**, *48*, 6177.

[59] A. M. Coclite, P. Lund, R. Di Mundo, F. Palumbo, *Polymer* **2013**, *54*, 24.

[60] H. Seong, K. Pak, M. Joo, J. Choi, S. G. Im, *Adv. Electron. Mater.* **2016**, *2*, 1500209.

[61] P. Kwong, S. Seidel, M. Gupta, *J. Vac. Sci. Technol. A* **2015**, *33*.

[62] B. Chen, P. Kwong, M. Gupta, *ACS Appl. Mater. Interfaces* **2013**, *5*, 12701.

[63] P. Kwong, C. A. Flowers, M. Gupta, *Langmuir* **2011**, *27*, 10634.

[64] Y. Yoo, B. G. Kim, K. Pak, S. J. Han, H. S. Song, J. W. Choi, S. G. Im, *ACS Appl. Mater. Interfaces* **2015**, *7*, 18849.

[65] A. M. Coclite, G. Ozaydin-Ince, F. Palumbo, A. Milella, K. K. Gleason, *Plasma Process. Polym.* **2010**, *7*, 561.

[66] J. Baek, J. J. Lee, M. Joo, D. Han, H. Kim, H. Seong, J. Kim, S. Yoo, S. Jeon, S. G. Im, *J. Mater. Chem. C* **2016**, *4*, 831.

[67] S. Janakiraman, S. L. Farrell, C. Y. Hsieh, Y. Y. Smolin, M. Soroush, K. K. S. Lau, *Thin Solid Films* **2015**, *595*, 244.

[68] C. D. Petruczok, K. K. Gleason, *Adv. Mater.* **2012**, *24*, 6445.

[69] C.-Y. Y. Hsieh, K. K. S. Lau, *Adv. Mater. Interfaces* **2015**, *2*, 1500341.

[70] C. Y. Wu, H. Y. Sun, W. C. Liang, H. L. Hsu, H. Y. Ho, Y. M. Chen, H. Y. Chen, *Chem. Commun.* **2016**, *52*, 3022.

[71] D. S. Bergsman, H. Zhou, S. F. Bent, *ECS Trans.* **2014**, *64*, 87.

[72] H. Zhou, J. M. Blackwell, H. B. Lee, S. F. Bent, *ACS Appl. Mater. Interfaces* **2013**, *5*, 3691.

[73] B. Waterkotte, F. Bally, P. M. Nikolov, A. Waldbaur, B. E. Rapp, R. Truckenmuller, J. Lahann, K. Schmitz, S. Giselbrecht, *Adv. Funct. Mater.* **2014**, *24*, 442.

[74] C. D. Petruczok, E. Armagan, G. O. Ince, K. K. Gleason, *Macromol. Rapid Commun.* **2014**, *35*, 1345.

[75] H. Goktas, X. Wang, N. D. Boscher, S. Torosian, K. K. Gleason, *J. Mater. Chem. C* **2016**, *4*, 3403.

**ADVANCED
SCIENCE NEWS**

www.advancedsciencenews.com

**ADVANCED
MATERIALS**

www.advmat.de

PROGRESS REPORT

[76] D. Bhattacharyya, K. Senecal, P. Marek, A. Senecal, K. K. Gleason, *Adv. Funct. Mater.* **2011**, *21*, 4328.

[77] D. Bhattacharyya, K. K. Gleason, *Chem. Mater.* **2011**, *23*, 2600.

[78] Y. Cao, A. E. Kovalev, R. Xiao, J. Kim, T. S. Mayer, T. E. Mallouk, *Nano Lett.* **2008**, *8*, 4653.

[79] H. Yoon, M. Chang, J. Jang, *Adv. Funct. Mater.* **2007**, *17*, 431.

[80] B. Reeja-Jayan, N. Chen, J. Lau, J. A. Kattirtzi, P. Moni, A. D. Liu, I. G. Miller, R. Kayser, A. P. Willard, B. Dunn, K. K. Gleason, *Macromolecules* **2015**, *48*, 5222.

[81] Q. Liu, H. Xu, K. K. S. Lau, G. Chen, in *Asia Pacific Confederation of Chemical Engineering Congress*, Engineers Australia, Melbourne, Australia **2015**, p. 1387.

[82] N. Chen, B. Reeja-Jayan, A. D. Liu, J. Lau, B. Dunn, K. K. Gleason, *Macromol. Rapid Commun.* **2016**, *37*, 446.

[83] D. S. Achilleos, T. A. Hatton, *J. Colloid Interface Sci.* **2015**, *447*, 282.

[84] W. S. O'Schaughnessy, S. K. Murthy, D. J. Edell, K. K. Gleason, *Biomacromolecules* **2007**, *8*, 2564.

[85] B. J. Kim, D. H. Kim, S. Y. Kang, S. D. Ahn, S. G. Im, *J. Appl. Polym. Sci.* **2014**, *131*, 40974.

[86] D. A. Spee, R. Bakker, C. H. M. Van Der Werf, M. J. Van Steenbergen, J. K. Rath, R. E. I. Schropp, *Thin Solid Films* **2011**, *519*, 4479.

[87] A. Perrotta, S. J. Garcia, M. Creatore, *Plasma Process. Polym.* **2015**, *12*, 968.

[88] J. H. Zhang, Y. S. Wang, J. H. Liang, D. S. Wuu, in *2015 International Symposium on Next-Generation Electronics*, IEEE, Piscataway, NJ, USA, **2015**.

[89] A. Behrendt, C. Friedenberger, T. Gahlmann, S. Trost, T. Becker, K. Zilberberg, A. Polywka, P. Gorrn, T. Riedl, *Adv. Mater.* **2015**, *27*, 5961.

[90] D. A. Spee, M. R. Schipper, C. H. M. van der Werf, J. K. Rath, R. E. I. Schropp, *Thin Solid Films* **2013**, *532*, 84.

[91] H. Seong, J. Choi, B. C. Jang, M. Kim, S. Yoo, S. Y. Choi, S. G. Im, *Adv. Electron. Mater.* **2016**, *2*, 1500385.

[92] B. C. Jang, H. Seong, S. K. Kim, J. Y. Kim, B. J. Koo, J. Choi, S. Y. Yang, S. G. Im, S.-Y. Choi, *ACS Appl. Mater. Interfaces* **2016**, *8*, 12951.

[93] J. Wang, X. W. Sun, Z. Jiao, *Materials* **2010**, *3*, 5029.

[94] C. A. Cutler, M. Bouguettaya, J. R. Reynolds, *Adv. Mater.* **2002**, *14*, 684.

[95] D. DeLongchamp, P. T. Hammond, *Adv. Mater.* **2001**, *13*, 1455.

[96] D. C. Borrelli, K. K. Gleason, *Macromolecules* **2013**, *46*, 6169.

[97] J. Baltazar, H. Sojoudi, S. A. Paniagua, S. Zhang, R. A. Lawson, S. R. Marder, S. Graham, L. M. Tolbert, C. L. Henderson, *Adv. Funct. Mater.* **2014**, *24*, 5147.

[98] H. Sojoudi, J. Baltazar, C. Henderson, S. Graham, *J. Vac. Sci. Technol. B* **2012**, *30*.

[99] J. Zang, S. Ryu, N. Pugno, Q. Wang, Q. Tu, M. J. Buehler, X. Zhao, *Nat. Mater.* **2013**, *12*, 321.

[100] H. Sojoudi, D. Chen, J. Y. Hong, J. Kong, R. E. Cohen, G. H. McKinley, K. K. Gleason, Unpublished.

[101] W. J. Jo, H. J. Kang, K. J. Kong, Y. S. Lee, H. Park, Y. Lee, T. Buonassisi, K. K. Gleason, J. S. Lee, *Proc. Natl. Acad. Sci. USA* **2015**, *112*, 13774.

[102] W. J. Jo, J. W. Jang, K. J. Kong, H. J. Kang, J. Y. Kim, H. Jun, K. P. S. Parmar, J. S. Lee, *Angew. Chem., Int. Ed.* **2012**, *51*, 3147.

[103] W. J. Jo, D. C. Borrelli, V. Bulović, K. K. Gleason, *Org. Electron.* **2015**, *26*, 55.

[104] J. Y. Kim, K. Lee, N. E. Coates, D. Moses, T. Q. Nguyen, M. Dante, A. J. Heeger, *Science* **2007**, *317*, 222.

[105] T. R. Cook, D. K. Dogutan, S. Y. Reece, Y. Surendranath, T. S. Teets, D. G. Nocera, *Chem. Rev.* **2010**, *110*, 6474.

[106] Y. Y. Smolin, S. Nejati, M. Bavarian, D. Lee, K. K. S. Lau, M. Soroush, *J. Power Sources* **2015**, *274*, 156.

[107] A. Perrotta, G. Aresta, E. R. J. J. van Beekum, J. Palmans, P. van de Weijer, M. M. C. M. R. van de Sanden, W. M. M. E. W. Kessels, M. Creatore, *Thin Solid Films* **2015**, *595*, 251.

[108] D. H. Kim, S. E. Atanasov, P. Lemaire, K. Lee, G. N. Parsons, *ACS Appl. Mater. Interfaces* **2015**, *7*, 3866.

[109] A. Ugur, F. Katmis, M. D. Li, L. J. Wu, Y. M. Zhu, K. K. Varanasi, K. K. Gleason, *Adv. Mater.* **2015**, *27*, 4604.

[110] H. Yan, Z. Chen, Y. Zheng, C. Newman, J. R. Quinn, F. Dotz, M. Kastler, A. Facchetti, *Nature* **2009**, *457*, 679.

[111] P. F. Moonen, I. Yakimets, J. Huskens, *Adv. Mater.* **2012**, *24*, 5526.

[112] M. K. Kwak, K. H. Shin, E. Y. Yoon, K. Y. Suh, *J. Colloid Interface Sci.* **2010**, *343*, 301.

[113] D. Qin, Y. Xia, G. M. Whitesides, *Nat. Protoc.* **2010**, *5*, 491.

[114] W. Z. Li, S. S. Xie, L. X. Qian, B. H. Chang, B. S. Zou, W. Y. Zhou, R. A. Zhao, G. Wang, *Science* **1996**, *274*, 1701.

[115] H. Chen, A. Roy, J.-B. Baek, L. Zhu, J. Qu, L. Dai, *Mater. Sci. Eng. R* **2010**, *70*, 63.

[116] D. N. Futaba, K. Miyake, K. Murata, Y. Hayamizu, T. Yamada, S. Sasaki, M. Yumura, K. Hata, *Nano Lett.* **2009**, *9*, 3302.

[117] M. C. Barr, R. M. Howden, R. R. Lunt, V. Bulović, K. K. Gleason, *Adv. Energy Mater.* **2012**, *2*, 1404.

[118] A. Izadi-Najafabadi, S. Yasuda, K. Kobashi, T. Yamada, D. N. Futaba, H. Hatori, M. Yumura, S. Iijima, K. Hata, *Adv. Mater.* **2010**, *22*, E235.

[119] K. K. S. Lau, J. Bico, K. B. K. Teo, M. Chhowalla, G. A. J. Amaratunga, W. I. Milne, G. H. McKinley, K. K. Gleason, *Nano Lett.* **2003**, *3*, 1701.

[120] M. De Volder, A. J. Hart, *Angew. Chem., Int. Ed.* **2013**, *52*, 2412.

[121] M. De Volder, S. H. Tawfick, S. J. Park, D. Copic, Z. Zhao, W. Lu, A. J. Hart, *Adv. Mater.* **2010**, *22*, 4384.

[122] S. Kim, H. Sojoudi, H. Zhao, D. Mariappan, G. H. McKinley, K. K. Gleason, A. J. Hart, *Sci. Adv.* **2016**, *2*, e1601660.

[123] M. Karaman, N. Cabuk, D. Ozyurt, O. Koysuren, *Appl. Surf. Sci.* **2012**, *259*, 542.

[124] C. D. Petruczok, H. J. Choi, S. Y. Yang, A. Asatekin, K. K. Gleason, G. Barbastathis, *J. Microelectromech. Syst.* **2013**, *22*, 54.

[125] H. Zhou, S. F. Bent, *ACS Appl. Mater. Interfaces* **2011**, *3*, 505.

[126] M. Ghaffari, S. Kosolwattana, Y. Zhou, N. Lachman, M. R. Lin, D. Bhattacharya, K. K. Gleason, B. L. Wardle, Q. M. Zhang, *Electrochim. Acta* **2013**, *112*, 522.

[127] C. D. O'Connell, M. J. Higgins, H. Nakashima, S. E. Moulton, G. G. Wallace, *Langmuir* **2012**, *28*, 9953.

[128] R. Brooke, D. Evans, M. Dienel, P. Hojati-Talemi, P. Murphy, M. Fabretto, *J. Mater. Chem. C* **2013**, *1*, 3353.